Study Report

VISUAL DETECTION OF PROTUBERANCE HAZARDS ON THE LUNAR SURFACE

15 August 1963

OFFICE OF SYSTEMS
OFFICE OF MANNED SPACE FLIGHT
NATIONAL AERONAUTICS AND SPACE ADMINISTRATION
WASHINGTON, D. C.

FOREWORD

In the course of studies leading to the development of the Contingency Plan for Project Apollo, it became apparent that visual recognition of lunar surface hazards was an important factor in determining the final landing point selection and approach mode for the LEM spacecraft. This study was initiated in May 1963 to provide quantitative information on the problem of visual detection of protuberance hazards on the lunar surface.

This report was prepared for the Office of Systems by the Systems Support Group as represented by the following members of the staff of the California Institute of Technology, Jet Propulsion Laboratory:

Robert R. Breshears
Lanny L. Lewyn

The assistance of Dr. Manfred Eimer, another member of the Systems Support Group, is greatfully acknowledged.

Charles W. Cole
Director, Systems Support Group

CONTENTS

TABLES

FIGURES

I. SUMMARY

A photometric model is presented which yields a luminance value for any sloping area of the lunar surface. This photometric model is applied to two extreme types of lunar surface protuberance hazards, cones and spheres. The photometric properties of these objects are then tested with experimentally derived photovisual threshold criteria. The results of these tests indicate the protuberance size which cannot be visually detected for various illumination conditions, viewing angles, and observer altitudes. It is apparent for earthshine lighting conditions and the majority of lunar equatorial landing areas of less than 60 degrees longitude that a significant fraction of protuberance hazards within the Apollo Lunar Excursion Module (LEM) horizontal maneuvering radius will probably not be visually detected from a hover altitude of 1,000 feet.

II. INTRODUCTION

The degree to which crew participation influences the choice of final landing point of a surface spacecraft on the Moon is influenced greatly by the ability of a pilot astronaut to relate observed appearance to objects which constitute a landing hazard. The problem of relating surface appearance to objects on the surface is one of pattern recognition and is beyond the scope of this work. However, before patterns can be recognized, luminance differences produced by surface protuberances must be large enough to be detected by the eye.

The ability of the eye to detect luminance differences relating to lunar surface features is dependent upon several parameters. Many of these parameters may be obtained by applying lunar photometry to model surface features. The results of the photometric analysis may then be subjected to photovisual threshold criteria to determine whether or not the model surface feature will produce sufficient contrast to be detected.

III. PHOTOMETRIC PROPERTIES OF THE LUNAR SURFACE

The luminance (B) of the lunar surface under conditions of normally incident illumination and viewing $\left(B_{o,o}\right)$ may be expressed by comparing that surface with a white lambert surface of luminance $B_{Lo,o}$ under similar conditions of illumination and viewing. The luminance ratio is given by the proportionality factor (ρ), the normal albedo.

$$\frac{B_{o,o}}{B_{Lo,o}} = \rho \tag{III–1}$$

The luminance of the lunar surface varies depending on the illumination and viewing geometry. This variation is described by introducing a second proportionality factor ϕ, the photometric function.

$$B = B_{o,o}\,\phi \tag{III–2}$$

This function is primarily dependent on the phase angle (g), the angle between the direction of incidence and the direction of emittance, and on $\propto$, the angle measured in the plane P, which contains g, from the direction of emittance to the intersection between the plane P and and the plane normal to P containing the normal to the local surface under observation. (Fig. 1) $\propto$ has positive values only when measured from the emitted ray in a direction away from the incident ray. The dependency of ϕ on $\propto$ and g is shown in Figures 2 and 3. (Ref. 1)

It may be shown that the luminance $B_{Lo,o}$ is related to the illumination by the proportionality factor π.

$$B_{Lo,o} = \frac{E}{\pi} \tag{III-3}$$

The above equations may be combined to yield an expression for the luminance of the lunar surface under all conditions of illumination and viewing .

$$B = \frac{E}{\pi}\rho\,\phi \tag{III-4}$$

IV. EVALUATION OF PHOTOMETRIC FUNCTION

In order to find the value of ϕ for a sloping area on the lunar surface, one must first determine g and $\propto$.

The phase angle (g) is independent of the local slope and may be expressed in terms of the three variables i', e' and θ', where i' is the angle formed by the incident ray and the vertical, e' is the angle formed by the emitted ray and the vertical, and θ' is the projection onto the horizontal plane of the phase angle g. (See Fig. 4.) g is then given by:

$$g = \cos^{-1}\,(1 + \cos\theta'\tan i'\tan e')\cos i'\cos e' \tag{IV-1}$$

$\propto$ may be expressed in terms of $\propto'$, the value for a horizontal surface and $\Delta\propto$, the incremental change in $\propto$ produced by tilting the surface:

$$\propto\; = \;\propto' + \Delta\propto \tag{IV-2}$$

where $|\propto'|$ is given by the equation:

$$|\propto'| = |\tan^{-1}\;[(\cos i'/\cos e') - \cos g]/\sin g\,| \tag{IV-3}$$

$\propto$ has positive values only when measured from the emitted ray in a direction away from the incident ray. The value of $\Delta\propto$ is dependent on the angle of slope (β) and the direction of slope. If the direction of slope is arranged to give a maximum value of $\Delta\propto$, holding β constant, then the relationship between β and $\Delta\propto$ is given by:

$$\Delta\propto\; = \tan^{-1}\;(\tan\beta/\cos\gamma) \tag{IV-4}$$

where γ is the angle between the vertical and the projection of the vertical on the plane containing g and is found from:

$$\gamma = \cos^{-1} (\cos e'/\cos \alpha') \tag{IV-5}$$

It may be shown that a ridge symmetrical about the vertical plane is oriented so as to produce maximum contrast if the ridge line is defined by the intersection of the horizontal plane and a plane normal to the plane containing the phase angle (g). This value of contrast is identical to the maximum contrast produced by a conical surface of similar slope at the same location.

Photometric function data is recorded in Tables I-V.

V. ILLUMINATION

The average illumination of the lunar surface from sunshine is $E_s = 1.52 \times 10^5$ cd/m^2. The average illumination $\left(E_m\right)$ of the lunar surface from earthshine may be calculated for any phase angle (G). (See Fig. 5.)

$$E_m = \int_A B_e \, \zeta \, (dA \cos e) \tag{V-1}$$

$$B_e = \frac{E_s}{\pi} \rho_e \cos i \quad \text{(lambert scattering)}^a \tag{V-2}$$

$$\zeta = 1/R^2 \tag{V-3}$$

$$\cos e = \cos \eta \cos \lambda \tag{V-4}$$

$$\cos i = \cos \kappa \cos \lambda \tag{V-5}$$

$$E_m = \int_{\left(G-\frac{\pi}{2}\right)}^{\frac{\pi}{2}} \int_{-\frac{\pi}{2}}^{\frac{\pi}{2}} \frac{r^2}{R^2} \frac{E_s}{\pi} \rho_e \cos^3 \lambda \cos \kappa \cos (G-\kappa) \, d\lambda d\kappa \tag{V-6}$$

$$E_m = \frac{r^2}{R^2} \frac{E_s}{\pi} \rho_e \frac{2}{3} \left[(\pi-G) \cos G + \sin G \right] \tag{V-7}$$

Assuming that the Earth scatters light like a lambert surface with an average normal albedo (ρ_e) of 0.4, E_m is tabulated for several values of G in Table VI.

---

[a] A law which incorporates forward scattering tendencies, such as that of Lommel-Seeliger, would be more appropriate. However, such laws must be fitted with empirically determined coefficients which are at this time uncertain.

VI. THRESHOLD CONTRAST DETECTION CAPABILITY OF THE HUMAN EYE

Many experiments have been conducted to measure the detection capability of the human eye. The largest body of data was taken by the Tiffany Foundation during World War II. Nineteen observers made more than 2 million observations of circular objects of 0.6 to 360 minutes in angular diameter, with contrasts both positive and negative and with and without binoculars. In addition to laboratory tests, field tests were also made to determine how well the laboratory results corresponded to field observations. The results, as reported by Blackwell (Ref. 2), are summarized in Figure 6. This Figure shows the contrast threshold (ϵ) as a function of angular diameter of the object and the background luminance for a 50% probability of detection in a single target field. The contrast threshold (ϵ) is defined as:

$$\epsilon = \frac{\text{object luminance} - \text{background luminance}}{\text{background luminance}} \tag{VI–1}$$

During his investigations, Blackwell found: (1) that the contrast threshold for detection was essentially the same for negative values of contrast as for positive values, (2) that use of binoculars did not increase the detectability of an object, (3) that the contrast threshold for a 95% probability of detection is approximately twice as large as for a 50% probability of detection, (4) for objects with angular diameters of less than 5 to 10 minutes of arc, that the product of contrast and area is constant for a given background luminance and probability of detection, as shown in Figure 6.

Holladay (Ref. 3) found a relationship between the contrast threshold for detection and the intensity of a glare source and the angle between the object and the glare source as shown below:

$$\epsilon' = \frac{B - B_o}{B_o + K\,E/(180\text{-}g)^2} \tag{VI–2}$$

where

ϵ' = effective contrast

B = object luminance (lumens sterad^{-1} meter^{-2})

B_o = background luminance (lumens sterad^{-1} meter^{-2})

K = 13.7 deg^2

E = glare source illuminance (candles meter^{-2})

g = phase angle (degrees)

ρ = normal albedo (0.065 for lunar maria areas)

But:

$$B = \frac{E}{\pi}\,\rho\,\phi \tag{VI–3}$$

$$B_o = \frac{E}{\pi} \rho \, \phi_o \tag{VI-4}$$

Therefore:

$$\epsilon' = \frac{\frac{E}{\pi} \rho \, \phi - \frac{E}{\pi} \rho \, \phi_o}{\frac{E}{\pi} \rho \, \phi_o + K \left[E/(180\text{-}g)^2\right]} \tag{VI-5}$$

$$\epsilon' = \frac{\phi - \phi_o}{\phi_o + K \, \pi/\rho \, (180\text{-}g)^2} \tag{VI-6}$$

The effective background luminance photometric function is:

$$\phi_o' = \phi_o + K \, \pi/\rho \, (180\text{-}g)^2 \tag{VI-7}$$

The effective background luminance is:

$$B_o' = \frac{E\rho}{\pi} \left[\phi_o + K \, \pi/\rho \, (180\text{-}g\right]^2 \tag{VI-8}$$

The tests of Lamar, Hecht, Shlaer, and Hendley (Ref. 4) showed that detectability depends on the area of an object and not on its shape. It was found that rectangles with width to length ratios up to 7:1 have the same detectability as circles with the same area.

Middleton (Ref. 5) performed experiments which showed the effect of a diffuse boundary on detection of objects. A limited number of experiments were conducted using binocular observations of a 2- by 3-deg field at a luminance level of about 30 $\text{sterad}^{-1}\text{m}^{-2}$. The variation in luminance across the boundary was given a probability function distribution as shown in Figure 7. The width of the boundary was defined as the distance between the point where the luminance starts to fall off to the point where the luminance is 1% of the total luminance difference above the background luminance. Figure 8 shows Middleton's results. Note that a boundary width of approximately 30 minutes or 1/6 the total object width increases the contrast threshold from approximately 0.017 to 0.11. Extrapolating Middleton's data to a boundary width ¼ of the total width (45 min) yields a contrast threshold (0.17) which is a factor of 10 larger than the threshold contrast for the same object with a sharp boundary. This factor will require modification for field sizes significantly different from that of the test target.

VII. CONE-SHAPED PROTUBERANCES

A. Analysis

The hazards of interest in this study differ somewhat from the objects used in the Tiffany tests. The targets used in the Tiffany tests exhibited a constant luminance which was either greater or less than the luminance of the surround. The luminance of a cone-shaped protuberance varies from a maximum value (B_H) greater than that of the horizontal surface to a minimum value (B_L) less than that of the horizontal surface (B_o). From the Tiffany data it is known that the contrast can be positive or negative and exhibit the same detectability. It is also known that, at least for relatively small objects, the contrast area product is constant for threshold detectability at a constant luminance. If two small targets have the same contrast area product and one of them exhibits constant luminance while the luminance of the other is spatially varied, then the constant luminance target should exhibit an ease of detection which is equal to or greater than that of the complex target. If the luminance B_H and the luminance B_L approximately satisfy the following relationship:[a]

$$B_H - B_o = B_o - B_L \qquad \text{(VII-1)}$$

then we may approximate the luminance, $B(\Omega)$, at any angle (Ω), (see Fig. 9) by:

$$B(\Omega) = B_o - \left(B_o - B_L\right) \cos \Omega \qquad \text{(VII-2)}$$

The contrast area product ($\epsilon A'$) may then be evaluated:

$$\epsilon A' = \int_A \left| \frac{B(\Omega) - B_o}{B_o} \right| dA \qquad \text{(VII-3)}$$

Substituting Equation VII-2,

$$\epsilon A' = \int_0^{2\pi} \left| \frac{\left[B_o - (B_o - B_L) \cos \Omega\right] - B_o}{B_o} \right| \frac{r_c^2}{2} \, d\Omega \qquad \text{(VII-4)}$$

which reduces to:

$$\epsilon A' = \frac{B_o - B_L}{B_o} \left(2 r_c^2\right) \qquad \text{(VII-5)}$$

The contrast area product (ϵA) of an object having the same radius r_c and constant contrast $\left(B_o - B_L\right)/B_o$ would be:

$$\epsilon A = \frac{B_o - B_L}{B_o} \left(\pi r_c^2\right) \qquad \text{(VII-6)}$$

[a] Note that this approximation is coarse at high object contrast but becomes better with decreasing contrast.

The ratio (a) of contrast area products for the two objects is just:

$$a = \frac{\epsilon A'}{\epsilon A} = \frac{2}{\pi} = 0.64 \qquad \text{(VII–7)}$$

If the contrast value $\epsilon = \left(B_o - B_L\right)/B_o$ is used for the conical object, then its area should be multiplied by $a = 0.64$ to yield a contrast area product which may be used with the Tiffany data. This number will vary with emittance angle (e'); however, the contrast value estimate should insure that the contrast area product is high.

If the height of the cone is h' and the slope is β, the area of the base (A) will be:

$$A = \pi\,(h'\tan\beta)^2 \qquad \text{(VII–8)}$$

The effective area of the base in the direction of the observer (Ae') will be:

$$A_e' = a\,\pi\,(h'\tan\beta)^2\ \cos e' \qquad \text{(VII–9)}$$

The effective visual angle subtended (Φ) is related to A_e' by:

$$A_e' = \pi\left[\frac{h\sin\frac{\Phi}{2}}{\cos e'}\right]^2 \qquad \text{(VII–10)}$$

Substituting Equation VII–9,

$$h' = \left(h\sin\frac{\Phi}{2}\right) / \left(\cos^{\frac{3}{2}} e'\ \tan\beta\right)(a)^{\frac{1}{2}} \qquad \text{(VII–11)}$$

For small Φ (measured in min):

$$h' = \frac{h\Phi}{2F}\cdot\frac{1}{\cos^{3/2} e'\ \tan\beta}\cdot\frac{1}{a^{1/2}} \qquad \text{(VII–12)}$$

where $F = 3.44 \times 10^2$ min/rad^{-1}.

The contrast value $\epsilon = \left(B_H - B_L\right)/B_o$ rather than $\left(B_o - B_L\right)/B_o$ is used with the Tiffany data to provide an optimistic bound which is equal to the maximum contrast found in the field of view.

This contrast value must be corrected for the glare of the source:

$$\text{(from Eq. VI–2)} \quad \epsilon' = \frac{B_H - B_L}{B_o + KE/(180 - g)^2} \qquad \text{(VII–13)}$$

The above expression reduces (see Eqs. VI–2 to VI–7) to:

$$\epsilon' = \frac{\phi_H - \phi_L}{\phi_o + K\pi/\rho\,(180 - g)^2} \qquad \text{(VII–14)}$$

To increase the detection probability from 50 to 95%, the contrast term must be halved.

$$\epsilon'' = \frac{\epsilon'}{2} \tag{VII-15}$$

Based on Middleton's diffuse boundary data, a hazard which is shaped like a cone except that the base is blended into the surface would be considerably more difficult to detect than a cone resting on a horizontal surface.

If it is assumed that the photometric function (ϕ) is a linear[a] function of surface slope, then the slope is proportional to the photometric function or the luminance. Therefore, integration of the luminance difference curve given in Figure 7 yields the form of the height versus radial distance. Using a diffuse boundary width of ¼ of the total object width (see Fig. 10), the decrease in effective contrast was assumed to be a factor of 10. The luminance versus radius and height versus radius profiles are shown in Figure 10. Note that the step difference in luminance across the top of the cone should not enhance its detectability since it occurs across zero area.

The contrast (ϵ''') corrected for the glare of the source, detection probability, and diffuse boundary is then:

$$\epsilon''' = \frac{\phi_H - \phi_L}{(2)\,(10)\left[\phi_o + K\,\pi/\rho\,(180 - g)^2\right]} \tag{VII-16}$$

In summary, the Tiffany data may be applied to the problem of detecting cone-shaped protuberances on the lunar surface by making the following assumptions:

1. The detectability of this object is the same as that for an object exhibiting a contrast of $(B_H - B_L)/10B_o$ and having an effective area equal to 0.64 of the base projected in the direction of observation. The factor of 10 in the contrast denominator is the diffuse boundary correction factor.
2. The background luminance and the denominator of the contrast term are modified by adding Holladay's glare factor.
3. To increase the probability of detection from 50 to 95% the contrast term should be halved.

B. Results

In Figures 11-14 the results of the cone-shaped protuberance analysis for a lunar maria area (ρ = 0.065) are expressed in terms of protuberance height (h'). This value of h' is the *minimum* value which would, in accordance with the analytical assumptions, exceed the photovisual threshold for contrast detection. The data is plotted in polar coordinate (r', θ') where r' is the normalized radial lunar surface dimension measured from the sub-observer point and θ is the direction of the radial dimension. Note that when $\theta' = 0$ degrees the radius r' points away

[a] Note that this approximation is coarse at high object contrast but becomes better with decreasing contrast.

from the Sun and when $\theta' = 180$ degrees the radius r' points toward the Sun. r' is normalized in such a way that $r' = 1$ corresponds to a surface distance exactly equal to the altitude of the observer above the mean surface.

It is possible to substitute another meaningful coordinate (e') for r'. If h represents the observer's altitude above the mean surface then $h \tan e'$ represents the radial surface distance, from the sub-observer point, of an object being viewed with an emittance angle e'. If this dimension is normalized by dividing the radial distance by h, $\tan e' = r'$. The plots are labeled with both e' and r' normalized radial dimensions.

Threshold height values (h') correspond to a value of $h = 1{,}000$ feet. For $h = x$, h' may be found by multiplying the value on the plot by $x/1{,}000$.

Note that for sunshine conditions the angle of incidence (i') values correspond to a given time of day. For earthshine conditions near the lunar equator i' is approximately equal to the selenenocentric longitude. Since Apollo LEM landing sites are limited to 60 degrees East and West longitude, earthshine i' values greater than 60 degrees are only of academic interest.

Other limitations which are discussed in the conclusions indicate that cones which have a height greater than that recorded on the plots may not be detectable. It is apparent (see Fig. 6) that for earthshine conditions, even at full Earth, the detectable heights are about an order of magnitude larger than the values obtained for sunshine.

In Figure 15, contours of constant h' are plotted. The value $h' = 1.6$ feet was chosen since it represents an Apollo LEM protuberance hazard. In the area outside the contours, protuberances of height $h' = 1.6$ feet are below threshold detectability.

VIII. SPHERICALLY SHAPED PROTUBERANCES

A. Analysis

Spherically shaped protuberances resting on the lunar surface are representative of a class of objects which are extremely easy to detect. They cast a high contrast shadow which has no diffuse boundary. Assuming that the shadow area provides the major part of the contrast area product, one needs to compute only the contrast exhibited by the shadow and the area of the shadow.

The contrast produced by the shadow uncorrected for glare is just:

$$\epsilon = \frac{B_o - B_s}{B_o} \qquad \text{(VIII-1)}$$

where

B_o is the luminance of the surround

B_s is the luminance of the shadow

Using Holladay's correction for the glare of the source:

$$\epsilon' = \frac{B_o - B_s}{B_o + KE/(180\text{-}g)^2} \tag{VIII-2}$$

The above expression reduces (See Eqs. VI–2 to VI–8) to:

$$\epsilon' = \frac{\phi_o - \phi_s}{\phi_o + K\pi/\rho(180\text{-}g)^2} \tag{VIII-3}$$

It is apparent that the area of the sphere in shadow will exhibit some residual luminance resulting from ground scattering; however, the conservative assumption $B_s = 0$ is made.

Then:

$$\epsilon' = \frac{\phi_o}{\phi_o + K\pi/\rho(180\text{-}g)^2} \tag{VIII-4}$$

The area of the ground shadow is just:

$$A_s = \frac{A_o}{\cos i'} \tag{VIII-5}$$

where A_o is the area of the shadow for normal illumination ($i' = 0$) which is easily shown to be:

$$A_o = \frac{\pi b'^2}{4} \tag{VIII-6}$$

where b' is the diameter of the sphere.

The area of the ground shadow (A_e) as seen from any observation angle e' will be:

$$A_e = A_s \cos e' f(g) = \frac{b'^2}{4} \frac{\cos e'}{\cos i'} f(g) \tag{VIII-7}$$

where the $f(g)$ term is introduced to account for the fact that the shadow is obscured by the object for phase angles less than 90 degrees and is given by:

$$g < 90 \qquad f(g) = \sin g \tag{VIII-8}$$

$$g > 90 \qquad f(g) = 1 \tag{VIII-9}$$

The shadow area (A_g) on the sphere as seen from any observation point with phase angle g (using the same nomenclature as in Fig. 5, replacing G with g) is:

$$A_g = \int_{-\frac{\pi}{2}}^{\left(g-\frac{\pi}{2}\right)} \int_{-\frac{\pi}{2}}^{\frac{\pi}{2}} \frac{b'^2}{4} \cos^2 \lambda \cos \eta \cos \eta \, d\lambda \, d\eta \qquad \text{(VIII–10)}$$

which reduces to:

$$A_g = \frac{\pi b'^2}{4} \cdot \frac{(1 - \cos g)}{2} \qquad \text{(VIII–11)}$$

The total shadow area (A_t) seen by the observer consists of the ground shadow and that portion of the sphere which is in shadow.

$$A_t = A_e + A_g = \frac{\pi b'^2}{4} \left[f(g) \cos e'/\cos i' + (1-\cos g)/2\right] \qquad \text{(VIII–12)}$$

The effective visual angle subtended (Φ) is related to A_t by:

$$A_t = \pi \left[\frac{b \sin \frac{\Phi}{2}}{\cos e'}\right]^2 \qquad \text{(VIII–13)}$$

Substituting Equation VIII–12:

$$b'^2 = \left[\frac{b \sin \frac{\Phi}{2}}{\cos e'}\right]^2 \frac{4}{[f(g) \cos e'/\cos i' + (1-\cos g)/2]} \qquad \text{(VIII–14)}$$

for small Φ (measured in min),

$$b' = \frac{b\,\Phi/F}{[f(g) \cos e'/\cos i' + (1-\cos g)/2]^{1/2} \cos e'} \qquad \text{(VIII–15)}$$

where $F = 3.44 \times 10^3$ min/rad.

In summary, the Tiffany data may be applied to the problem of detecting spherically shaped protuberances resting on the lunar surface by making the following assumptions:

1. The detectability of this object is the same as that for an object exhibiting a contrast of $\epsilon = B_o/B_o = 1$ and having an effective area equal to the sum of the projected ground shadow and the area of the sphere in shadow. The contribution of the portion of the sphere not in shadow to the contrast area product is assumed to be small and to be slightly offset by the conservative assumption that $B_s = 0$.
2. The background luminance and the denominator of the contrast term ground luminance are modified by adding Holladay's glare factor.

3. To increase the probability of detection from 50 to 95% the contrast term should be halved.

B. RESULTS

In Figures 16-20 the results of the spherically shaped protuberances analysis for a lunar maria area (ρ = 0.065) are expressed in terms of protuberance height h'. This value of h' is the minimum value which would, in accordance with the analytical assumptions, exceed the photo-visual threshold for contrast detection. Other limitations which are discussed in the conclusions imply that spheres which have a height greater than that recorded on the plots may not be detectable. It is apparent (see Fig. 6) that, for earthshine conditions, even at full Earth, the detectable heights are about an order of magnitude larger than the values obtained for sunshine.

In Figure 21 contours of constant h' are plotted. The value h' = 1.6 feet was chosen since it represents an Apollo LEM protuberance hazard. In the area outside the contours protuberances of height h' = 1.6 feet are below threshold detectability.

IX. CONCLUSIONS

The two model protuberance hazards that were chosen for study represent reasonable extremes of detection difficulty. Therefore, the contrast threshold detection of typical lunar protuberances will, with high probability, represent a degree of difficulty which is bounded by the detectability of model hazards. Until reconnaissance missions are performed or more exact theoretical determinations of lunar protuberance shapes are made, one is bound to favor the conservative model, the cone. Naturally, the conservative conical protuberance model analysis yields threshold protuberance heights (h') which are in most cases a factor of 2 to 7 times higher than the values obtained for the spherical protuberance model. However, in order to put these results in proper perspective, it is necessary to discuss those factors which, in most instances, influence the threshold numbers.

A. PHOTOMETRIC FACTORS

1. Under earthshine conditions, contrast detectability varies strongly with illumination. In the earthshine calculations the optimistic assumptions of both full Earth and an albedo of 0.4 were made.
2. Although cones or dunes with 8-deg slopes are possible Apollo LEM hazards, the optimistic choice of cones with 15-deg slopes was made for the conical protuberance calculations. A more diffuse base boundary would significantly reduce the conical protuberance detectability.

B. PHOTOVISUAL FACTORS

1. The threshold detection ability of an observer will be reduced in the process of detecting an object in a wide and complex field. Smith (Ref. 6) reports that contrast

detectability decreases sharply with increasing object angle as measured from the optical axis and that this peripheral detectability may be enhanced by allowing the observer to use visual aids such as binoculars.

2. The threshold detection ability of an observer will be affected by the time alloted for observation. Krendel and Wodinsky (Ref. 7) have shown that the percentage of objects which may be detected in a complex field is an exponential function of time.
3. Threshold detection probability may be affected considerably by risks and rewards involved in the detection process.
4. The threshold detection ability of an observer will be reduced if he is not dark-adapted at the time of the observation.

For most sunshine illumination conditions it is apparent that either protuberance hazard will produce detectable luminance differences within the horizontal maneuvering radius of the LEM. The ability of an observer to relate observed luminance differences to hazardous protuberance height is a difficult problem in pattern recognition.

However, for most earthshine conditions, even at full Earth, it is apparent that the ability of an observer to detect, from the hover altitude, luminance differences produced by protuberances within the maneuvering radius of the LEM is somewhat restricted. This restriction is significant for conical protuberances at lunar equatorial longitudes less than 50 degrees. Similarly, detection of spherically shaped protuberances is somewhat restricted at lunar equatorial longitudes less than 30 degrees. A significant fraction of critical protuberance hazards ($b' = 1.6$ ft) within the LEM horizontal maneuvering radius will probably not be detected from the hover altitude in the central portion of the Moon's visible disc.

NOMENCLATURE

A. Illumination

E	Illumination factor (all values in cd/m^2).
E_s	Illumination of lunar surface from sunshine.
E_m	Illumination of lunar surface from earthshine.

B. Albedo

ρ	Normal albedo.
ρ_e	Normal albedo of Earth cloud cover.

C. Luminance

B	Luminance (all values in lumens sterad^{-1} meter^{-2}).
$B_{o,o}$	Luminance of surface under normal conditions of illumination and viewing.
$B_{Lo,o}$	Luminance of white lambert surface under conditions of normal illumination and viewing.
B_o	Luminance of horizontal background.
B_o'	Luminance of horizontal background corrected for glare.
B_s	Luminance of shadow area.
B_H	Maximum luminance of surface with luminance greater than that of horizontal surface.
B_L	Minimum luminance of surface with luminance less than that of horizontal surface.

D. Angles

g	Photometric phase angle (see Figs. 1 and 4).
G	Photometric phase angle (see Fig. 5).
α	Auxiliary angle used in determining value of photometric function of any surface.
α'	Auxiliary angle used in determining value of photometric function of horizontal surface.
$\Delta\alpha$	Change in α produced by tilting surface from horizontal.
γ	Angle from vertical to projection of vertical on plane of phase angle.
β	Angle of local surface tilt with respect to horizontal.
ζ	Solid angle subtended by a surface of unit area located at a distance R (R^2 measured in same units as area).

i	Photometric angle of incidence measured from normal to local surface (see Fig. 1).
i'	Photometric angle of incidence measured from vertical (see Fig. 4).
e	Photometric angle of emission measured from normal to local surface (see Fig. 1).
e'	Photometric angle of emission measured from vertical (see Fig. 4).
θ'	Projection of phase angle onto horizontal plane. (see Fig. 4).
η	Auxiliary photometric angle (see Fig. 5).
κ	Auxiliary photometric angle (see Fig. 5).
l	Auxiliary photometric angle (see Fig. 5).
Ω	Auxiliary angle used in computation of contrast-area product (see Fig. 9).
Φ	Angle subtended by threshold contrast target (min)
μ	Angle subtended by diffuse boundary (min)
F	Angular conversion factor (3.44×10^2 min/rad)
K	Glare angular correction factor (13.7 $\deg^2$)

E. Photometric Function

ϕ	Photometric function.
ϕ_o	Photometric function for horizontal surface.
ϕ_o'	Photometric function for horizontal surface corrected for glare.
ϕ_H	Photometric function for surface with luminance greater than that of horizontal surface.
ϕ_L	Photometric function for surface with luminance less than that of horizontal surface.

F. Distance

R	Distance from Earth to mean lunar orbit.
h	Height of observer above lunar surface.
h'	Minimum value of protuberance height which would, in accordance with the analytical assumptions, exceed the photovisual contrast threshold.
r_e	Radial distance from center of cone.
r_c	Base radius of conical protuberance.
r'	Normalized radial distance from sub-observer point.

G. Contrast

ϵ	Contrast.

ϵ' Contrast corrected for glare.

ϵ'' Contrast corrected for glare and detection probability.

ϵ''' Contrast corrected for glare, detection probability, and diffuse boundary.

$\epsilon A'$ Contrast area product for cones.

ϵA Contrast area product for discs.

H. Area

A' Effective area of base of cone.

A Base area of cone.

A'_ϵ Effective area of cone projected in direction of emittance.

A_s Area of ground shadow.

A_o Area of ground shadow for normal illumination.

A_e Area of ground shadow projected in direction of emittance.

A_g Shadow area of sphere for any phase angle.

A_t Total shadow area projected in direction of emittance.

a Effective area correction factor.

BIBLIOGRAPHY

1. "Ranger Preflight Science Analysis and the Lunar Photometric Model", Herriman, A. G., Washburn, H. W., Willingham, D. E., TR No. 32-384 (Rev.); Jet Propulsion Laboratory, California Institute of Technology, Pasadena, California; Revised March 11, 1963.

2. "Contrast Thresholds of the Human Eye", Blackwell, H. R., *Journal of the Optical Society of America,* 36: 624-643.

3. "The Fundamentals of Glare and Visibility", Holladay, L.L., *Journal of the Optical Society of America,* 12.271-319, 1926.

4. "Size, Shape, and Contrast in Detection of Targets by Daylight Vision. I. Data and Analytical Description",Lamar, E.S., Hecht, S.S., Shlaer, S., Hendley, C.D., *Journal of the Optical Society of America,* 37: 531-554, 1947.

5. "Vision Through the Atmosphere", Middleton, W.E.K., University of Toronto Press, 1958 (p. 92).

6. "Use of Binoculars in Search for Submarines", Smith, R.P., *Visual Search Techniques,* National Academy of Sciences - National Research Council, Publication 712 (pp. 32-40).

7. "Visual Search in Unstructured Fields", Krendel, E.S., and Wodinsky, J., *Visual Search Techniques,* National Acadamy of Sciences - National Research Council, Publication 712 (pp. 151-169).

Table I

PHOTOMETRIC PARAMETERS FOR $i' = 70$ AND $\beta = 15^{\circ}$

ϵ'	θ'	g	α'	γ	$\Delta\alpha$	ϕ_H	ϕ_o	ϕ_L
0	0	70	0	0	15	0.19	0.14	0.043
	30							
	60							
	90							
	120							
	150							
	180							
30	0	40	30	0	15	0.30	0.17	0.05
	30							
	60							
	90	73	- 5	30	17	0.20	0.15	0.06
	120							
	150							
	180	100	-30	0	15	0.12	0.07	0.02
45	0	25	45	0	15	0.43	0.21	0.07
	30							
	60							
	90							
	120							
	150							
	180	115	-45	0	15	0.09	0.06	0.02
60	0	10	60	0	15	0.54	0.39	0.11
	30	29	22	58	26	0.48	0.35	0.16
	60	55	- 7	60	28	0.33	0.16	0.11
	90	80	-28	56	25	0.20	0.16	0.09
	120	104	-44	47	21	0.14	0.10	0.04
	150							
	180	130	-60	0	15	0.08	0.05	0.02
70	0	0	70	0	15	1.0	1.0	1.0
	30	28	-14	70	38	0.56	0.50	0.37
	60	56	-27	67	34	0.36	0.31	0.22
	90	83	-42	63	30	0.22	0.17	0.10
	120	109	-54	54	25	0.14	0.08	0.04
	150	130	-65	37	18	0.09	0.06	0.02
	180	140	-70	0	15	0.06	0.04	0.01

Table II

PHOTOMETRIC PARAMETERS FOR $i' = 60$ AND $\beta = 15^\circ$

ϵ'	θ'	g	α'	γ	$\Delta\alpha$	ϕ_H	ϕ_o	ϕ_L
0	0	60	0		15	0.26	0.22	0.12
	30							
	60							
	90							
	120							
	150							
	180							
30	0	30	30	0	15	0.39	0.29	0.15
	30	36	21	21	16	0.40	0.30	0.16
	60	50	6	21	17	0.32	0.28	0.16
	90	64	- 9	29	17	0.24	0.21	0.14
	120							
	150	86	-27	13	15	0.16	0.13	0.08
	180	90	-30	0	15	0.15	0.12	0.08
45	0	15	45	0	15	0.52	0.39	0.22
	30	28	21	41	20	0.47	0.37	0.22
	60	49	- 5	44	21	0.35	0.31	0.20
	90	70	-21	41	20	0.25	0.21	0.16
	120	87	-33	32	17	0.17	0.14	0.08
	150	99	-42	20	16	0.14	0.10	0.06
	180	105	-45	0	15	0.13	0.1	0.06
60	0	0	60	0	15	1.0	1.0	1.0
	30	26	-13	60	28	0.57	0.52	0.44
	60	51	-26	56	26	0.37	0.34	0.28
	90	76	-38	38	19	0.24	0.21	0.18
	120	83	-41	47	22	0.21	0.18	0.13
	150	114	-57	21	17	0.19	0.08	0.06
	180	120	-60	0	15	0.11	0.08	0.04
70	0							
	30							
	60							
	90							
	120	104	-60	46	21	0.16	0.14	0.09
	150	122	-67	29	17	0.11	0.08	0.05
	180	130	-70	0	15	0.95	0.07	0.04

Table III

PHOTOMETRIC PARAMETERS FOR $i' = 50$ AND $\beta = 15^\circ$

ϵ'	θ'	g	α'	γ	$\Delta\alpha$	ϕ_H	ϕ_o	ϕ_L
0	0	50	0	0	15	0.33	0.3	0.2
	30							
	60							
	90							
	120							
	150							
	180							
30	0	20	30	0	15	0.51	0.44	0.27
	30	27	18	25	16	0.48	0.42	0.29
	60	44	- 1	30	17	0.38	0.35	0.25
	90	55	-13	28	17	0.32	0.28	0.23
	120							
	150							
	180	90	-30	0	15	0.15	0.12	0.08
45	0	5	45	0	15	0.78	0.78	0.75
	30	22	- 2	45	21	0.56	0.43	0.44
	60	43	-15	43	20	0.41	0.37	0.31
	90	63	-27	38	19	0.29	0.26	0.22
	120	79	-34	28	18	0.21	0.19	0.14
	150	91	-43	16	16	0.17	0.15	0.12
	180	95	-45	0	15	0.16	0.13	0.10
60	0	10	60				0.38	
	30							
	60							
	90	71	-25				0.20	
	120							
	150							
	180	110	-60				0.11	
70	0							
	30							
	60							
	90							
	120							
	150							
	180							

Table IV

PHOTOMETRIC PARAMETERS FOR $i' = 40$ AND $\beta = 15°$

ϵ'	θ'	g	α'	γ	$\Delta\alpha$	ϕ_H	ϕ_o	ϕ_L
0	0	40	0	0	15	0.41	0.38	0.30
	30							
	60							
	90							
	120							
	150							
	180							
30	0	10	30	0	15		0.62	
	30							
	60							
	90							
	120							
	150							
	180	70	-30	0	15		0.22	
45	0	5	-45	0	15		0.93	
	30	21	- 8				0.56	
	60	40	-26				0.42	
	90	57	-33				0.33	
	120	72	-39				0.22	
	150	81	-43				0.18	
	180	85	-45	0	15		0.17	
60	0	20	-60	0	15	0.70	0.67	0.64
	30							
	60							
	90	68	-51				0.26	
	120							
	150							
	180	100	-60	0	15	0.16	0.14	0.12
70	0	30	-70		15			
	30							
	60							
	90							
	120							
	150	105	-69	19	16	0.16	0.14	0.11
	180	110	-70	0	15	0.14	0.13	0.10

Table V

PHOTOMETRIC PARAMETERS FOR $i' = 30$ AND $\beta = 15^\circ$

ϵ'	θ'	g	α'	γ	$\Delta\alpha$	ϕ_H	ϕ_o	ϕ_L
0	0	30	0					
	30							
	60							
	90							
	120							
	150							
	180							
30	0	0					1	
	30	15	- 7				0.63	
	60	29	-15				0.50	
	90	41	-21				0.4	
	120	51	-26				0.33	
	150	58	-29				0.30	
	180	60	-30				0.28	
45	0	15	-45				0.72	
	30	23	-38				0.60	
	60	38	-35				0.46	
	90	52	-38				0.35	
	120	64	-39				0.27	
	150	72	-43				0.23	
	180	75	-45				0.22	
60	0	30	-60				0.56	
	30							
	60							
	90	64	-55				0.30	
	120							
	150							
	180	90	-60				0.17	

Table VI

EARTHSHINE ILLUMINATION VALUES (E_m) FOR SEVERAL EARTH PHASE ANGLES (G)

E_m (cd/m^{-2})	G (deg)
11.4	0
10.1	30
7.0	60
3.6	90
1.2	120
.17	150

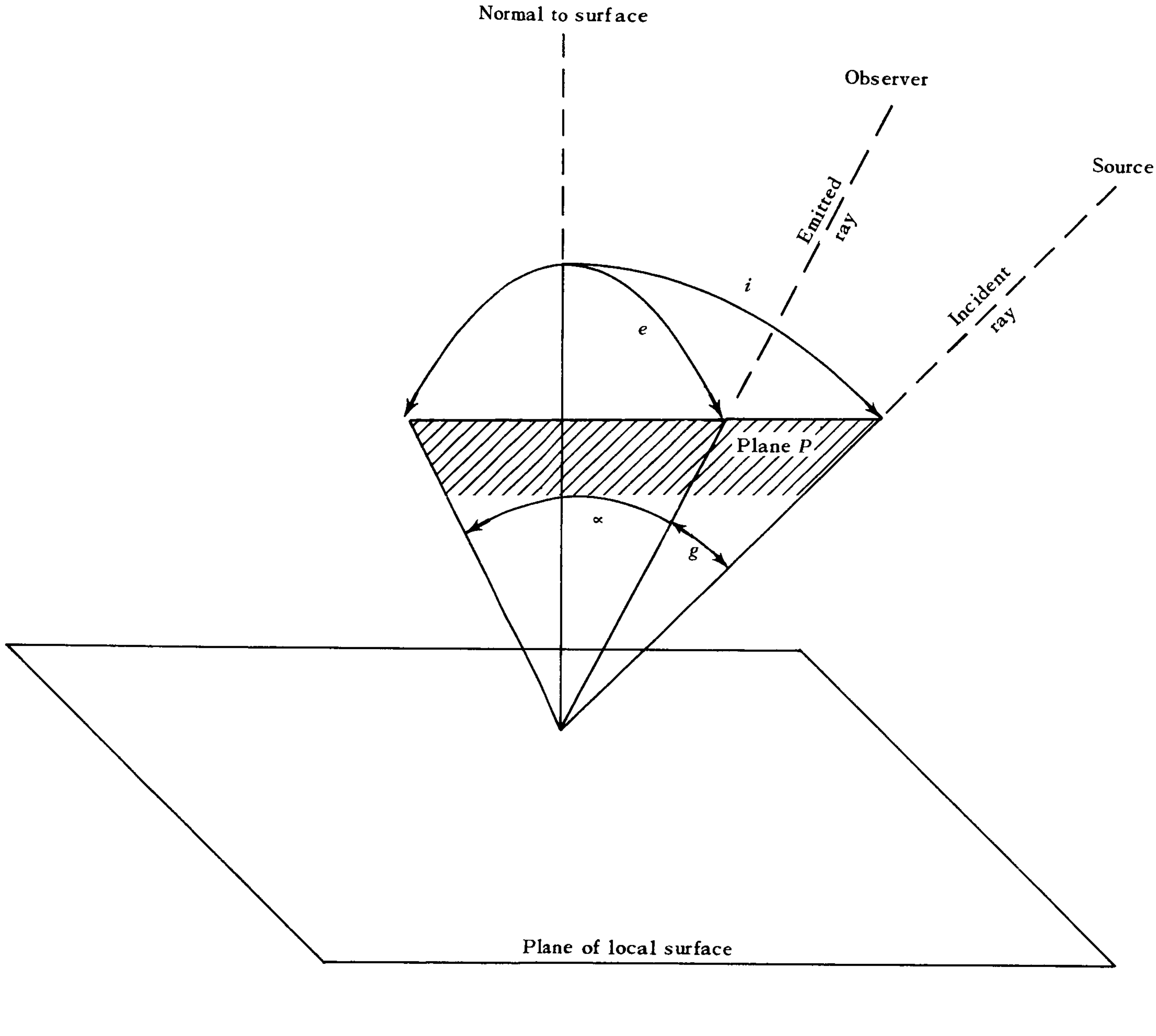

Figure 1. General Photometric Angles

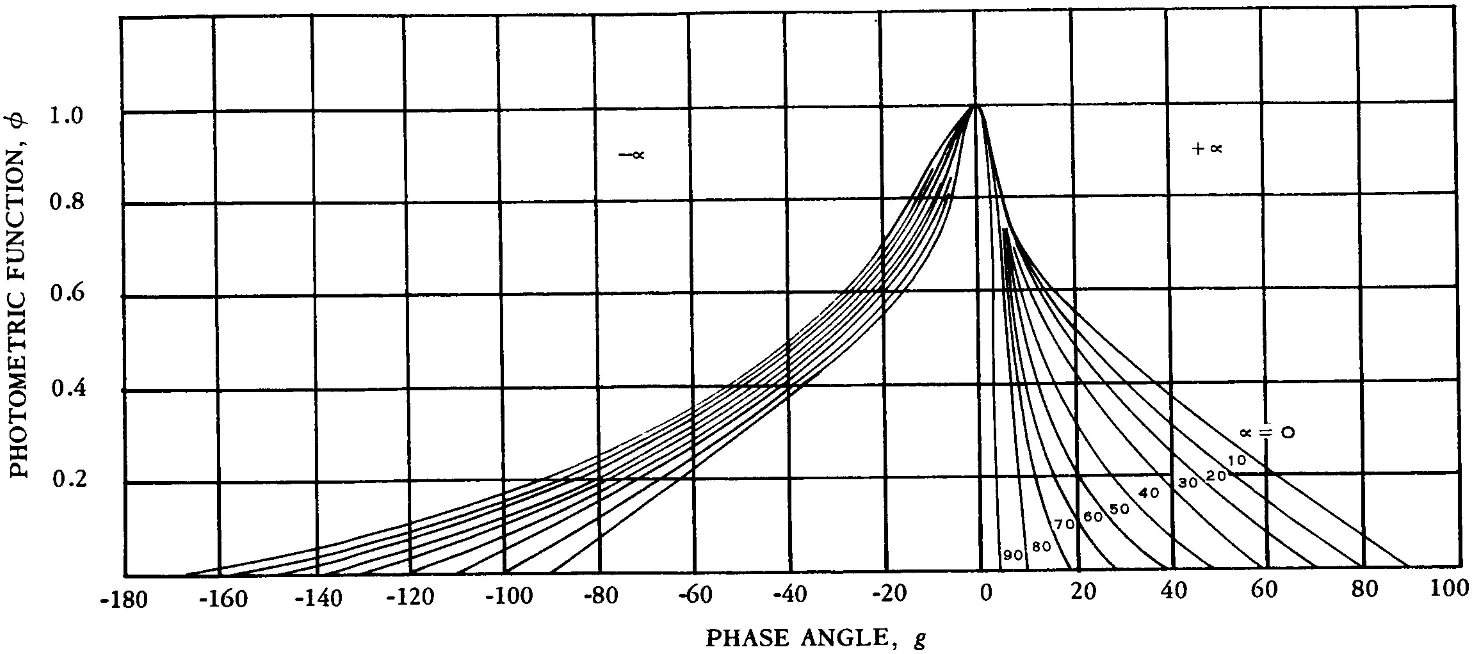

Figure 2. Photometric Function Vs g

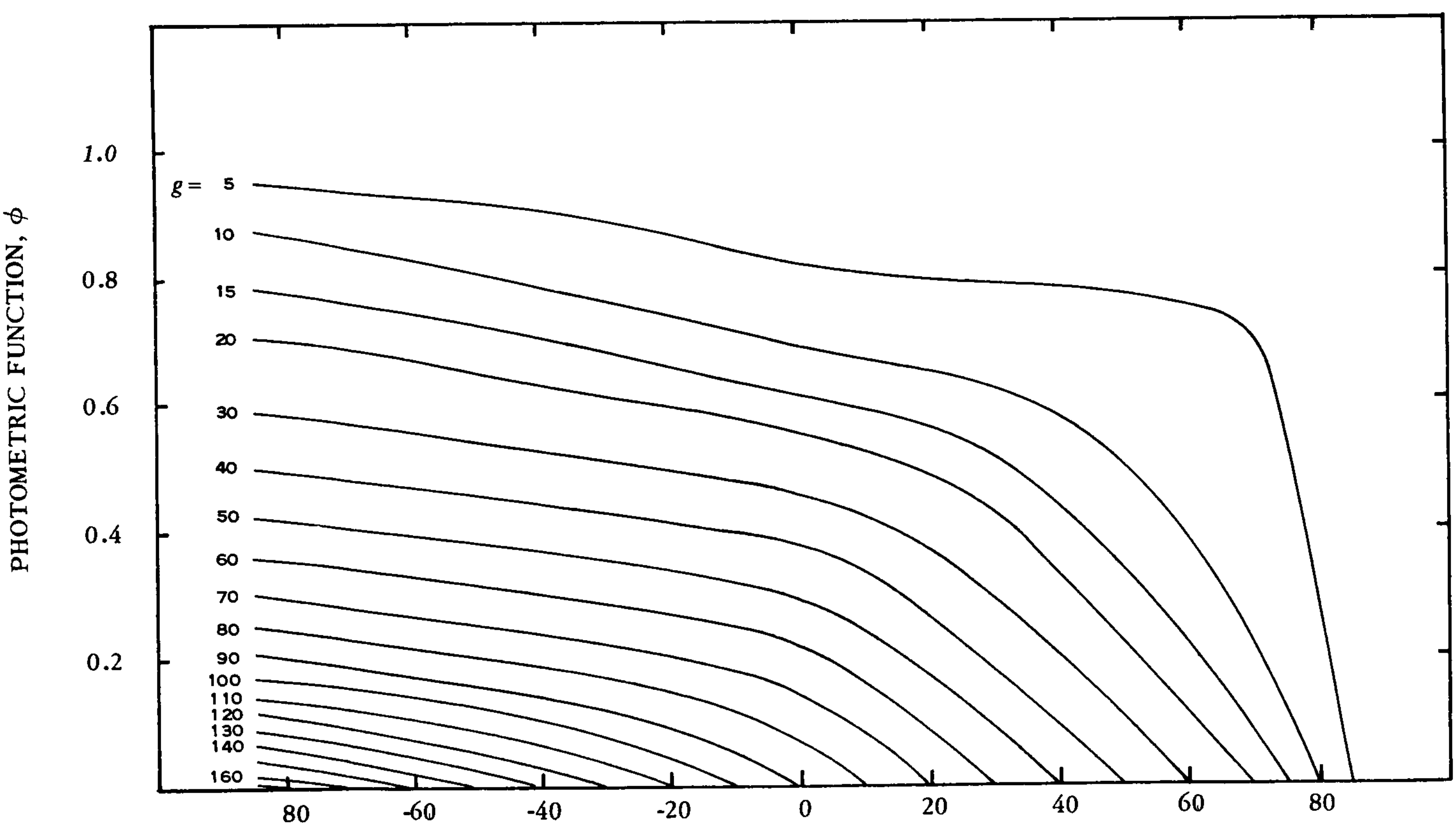

Figure 3. Photometric Function Vs $\propto$

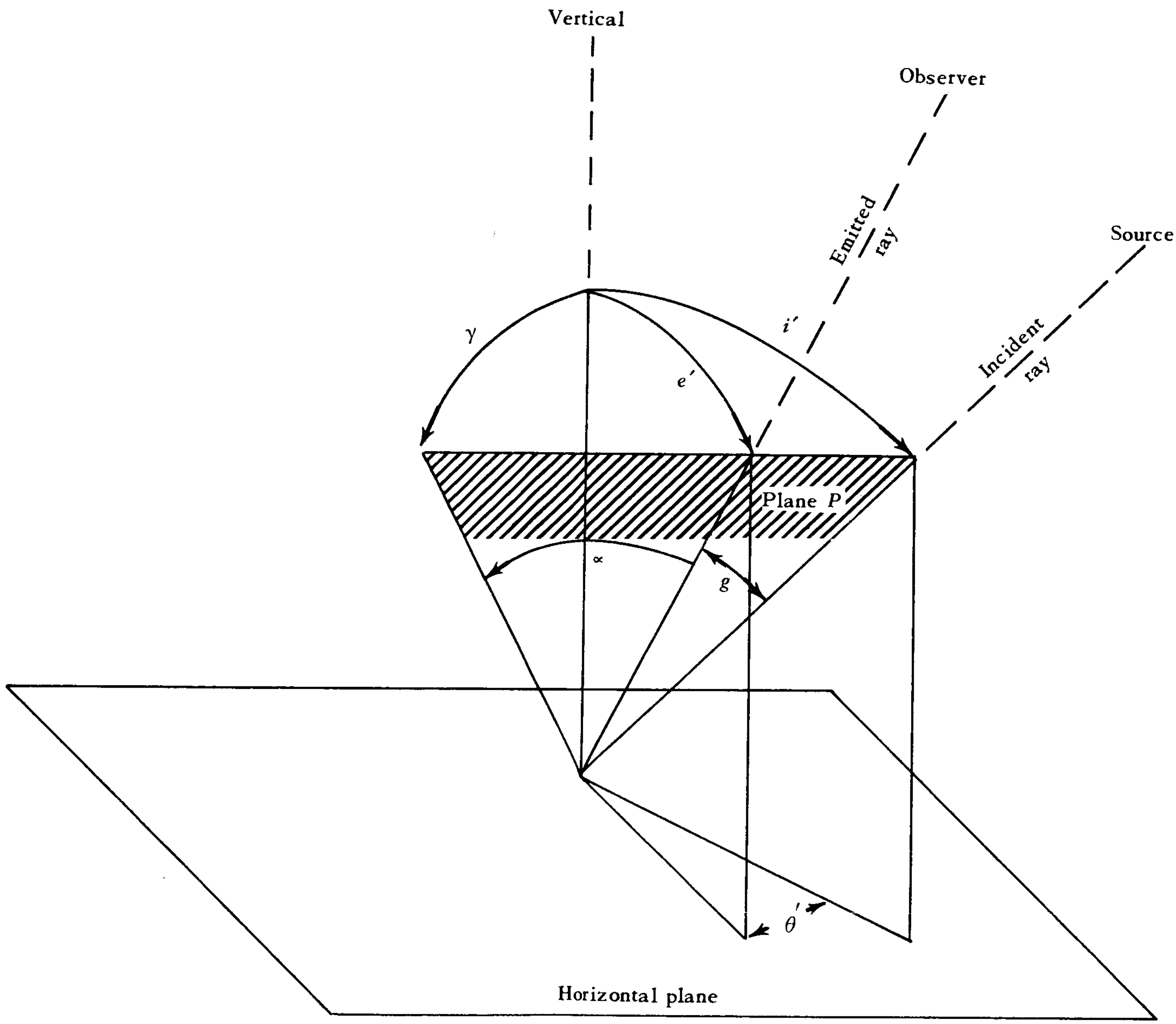

Figure 4. Special Photometric Angles

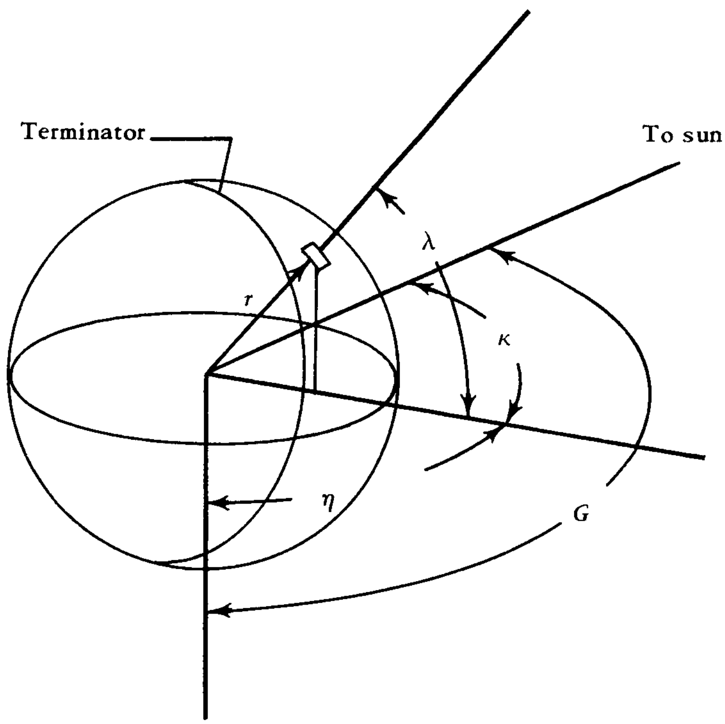

Figure 5. Earthshine Illumination Angles

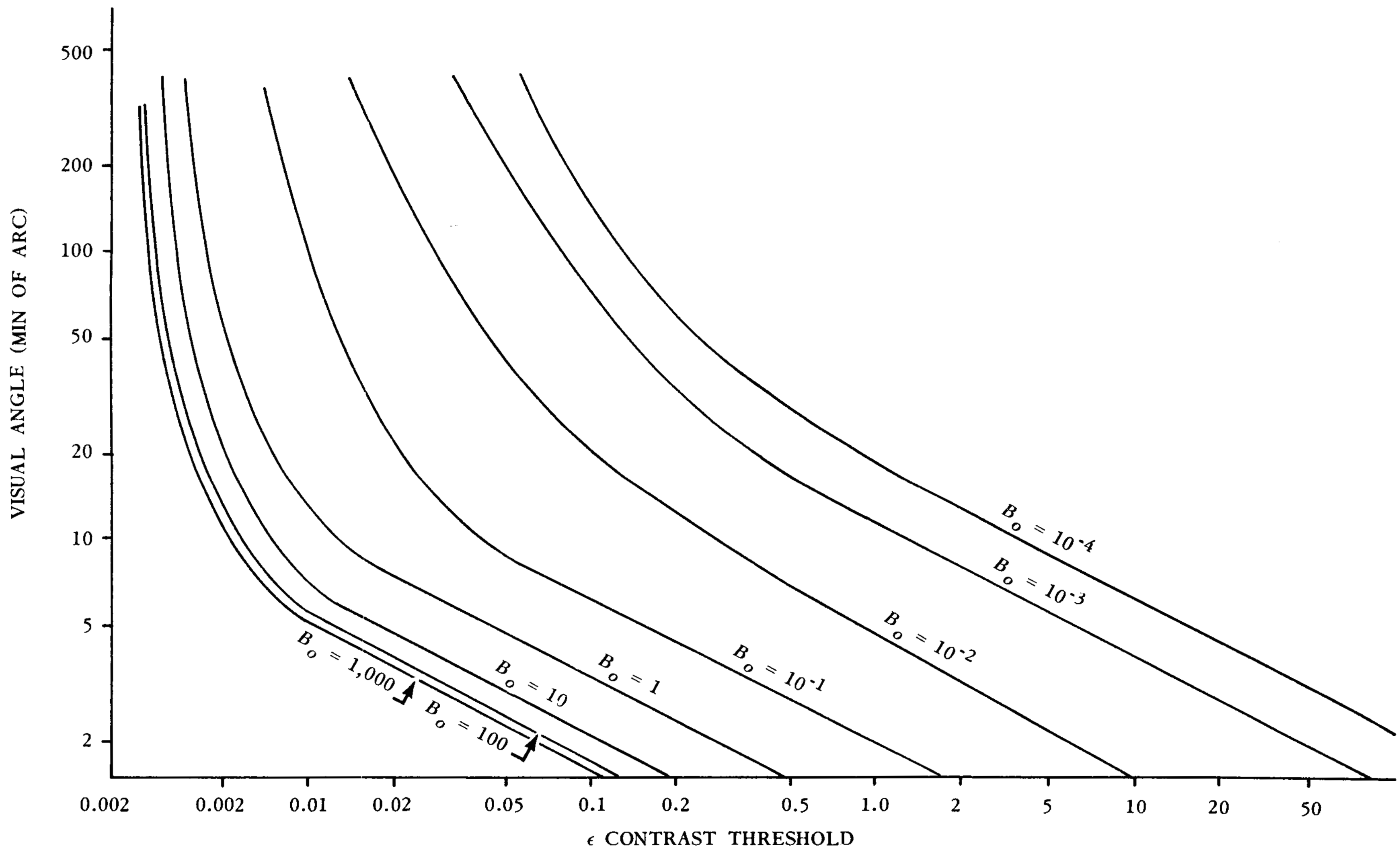

Figure 6. Visual Detection Threshold As Function of Contrast, Object Size, and Luminance

1. Circular objects.
2. 50% probability of detection.
3. Sharp boundary between object and background.
4. Background luminance = B_o (cd/m^{-2}).
5. $\epsilon = (B - B_o)/B_o$; B = object luminance.
6. From Ref. 2.

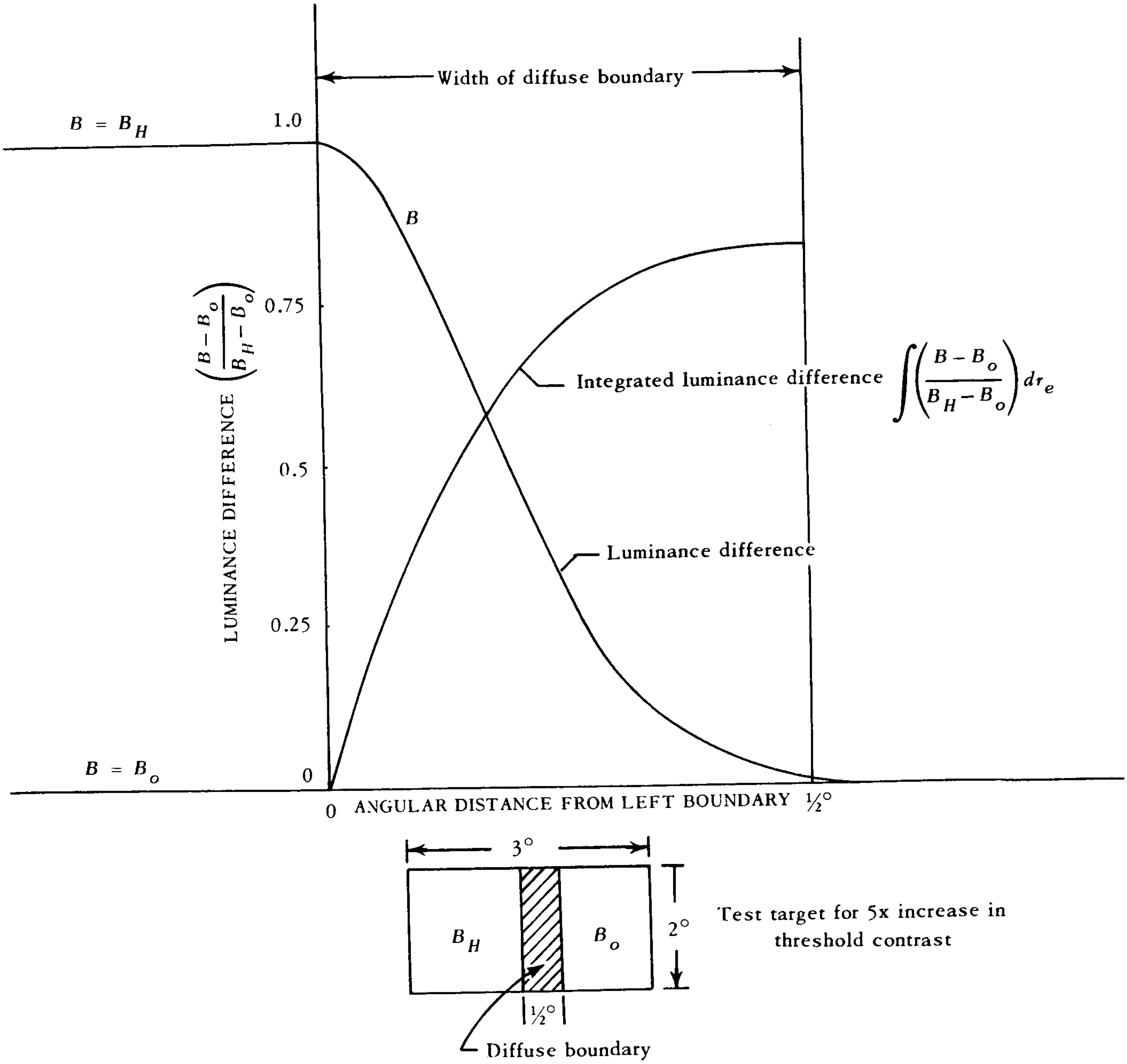

Figure 7. Probability Curve Used by Middleton for Luminance of Diffuse Boundary

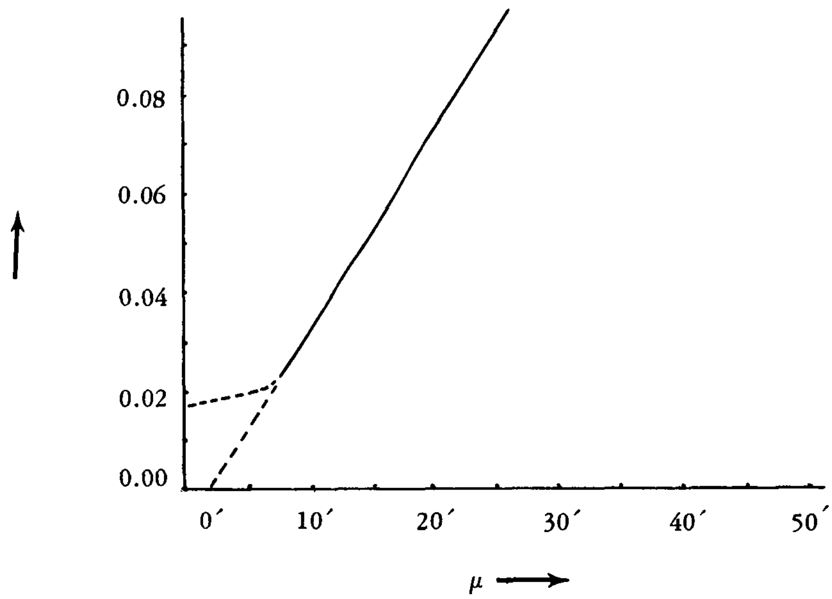

Figure 8. Variation of Threshold Contrast With Width (μ) of a Diffuse Boundary

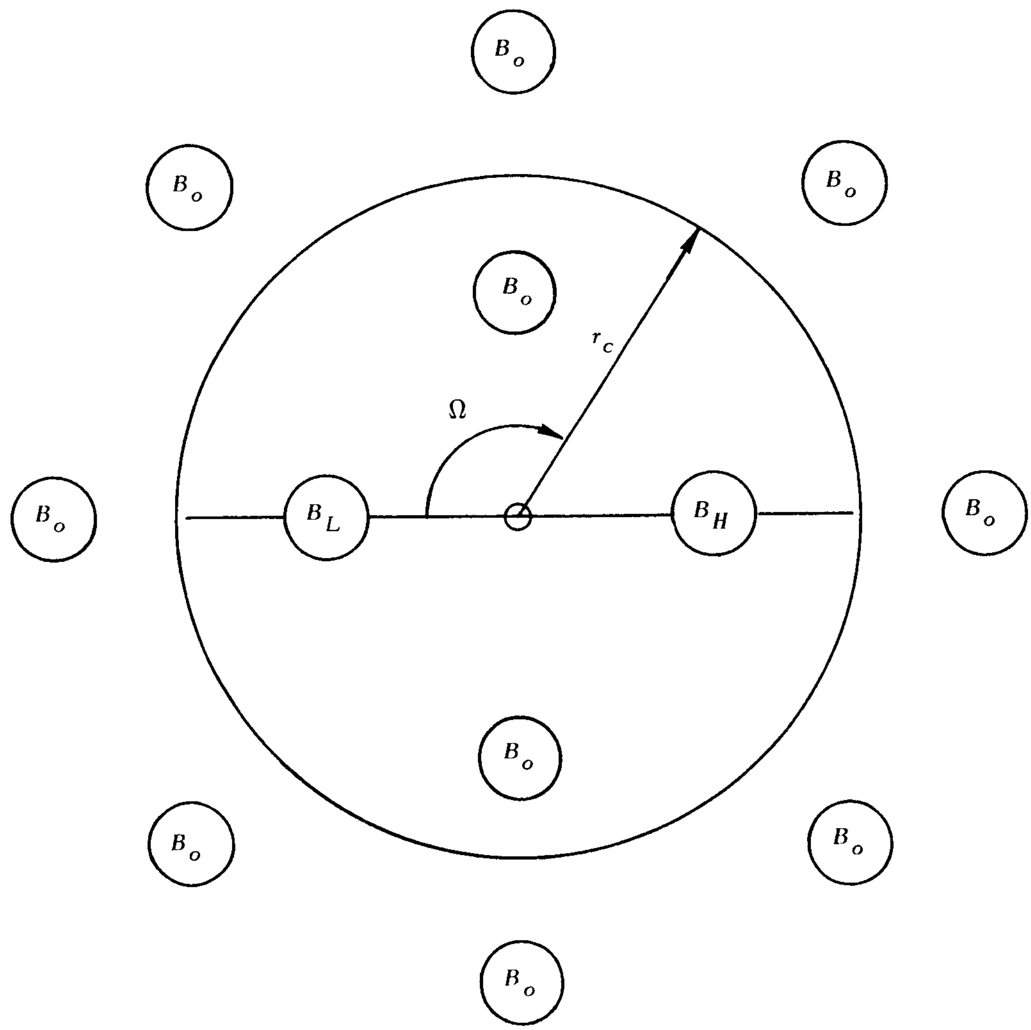

Figure 9. Coordinate System Used for Determination of Conical Protuberance Contrast Area Product

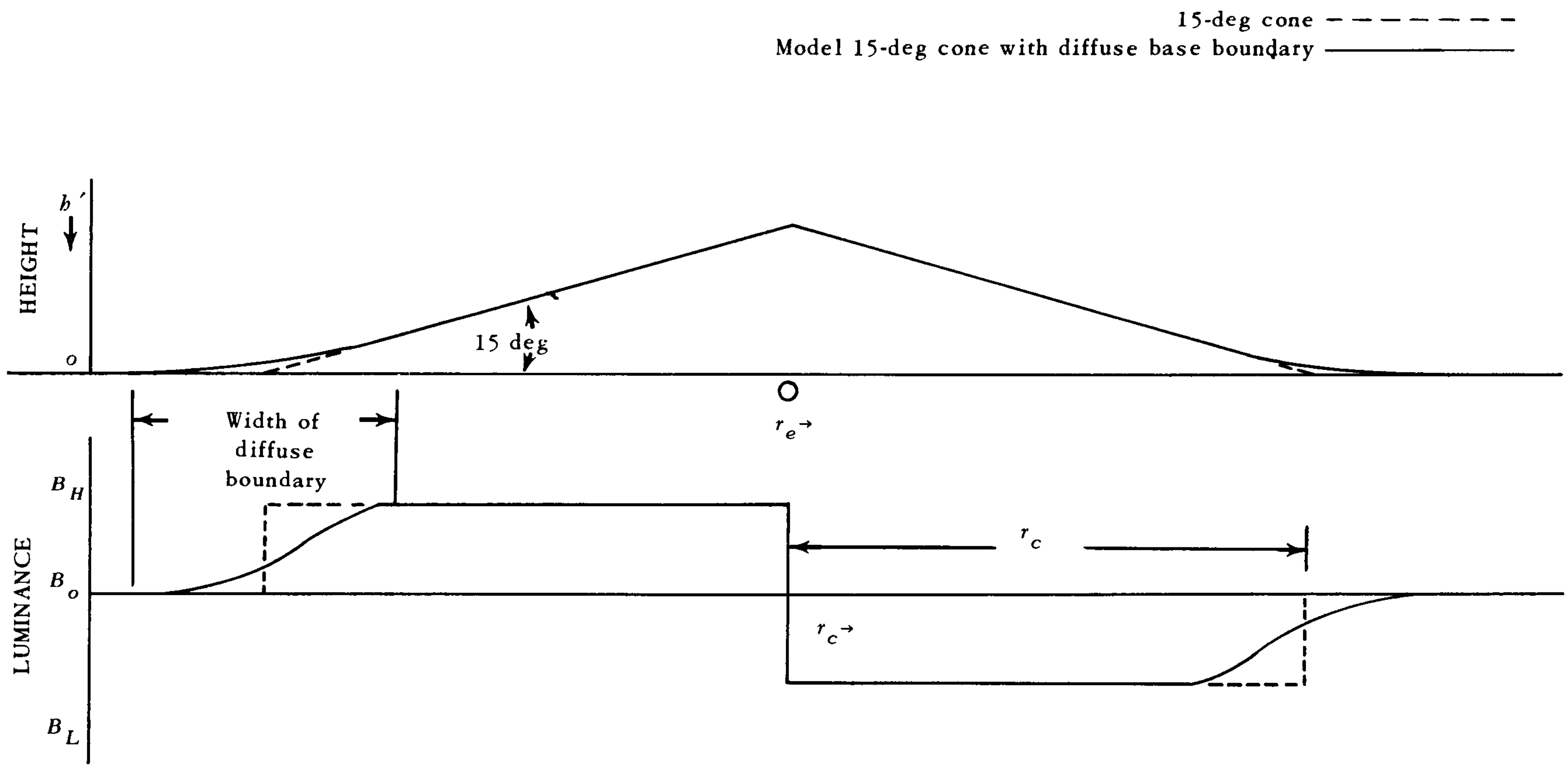

Figure 10. Luminance and Height Profiles of Conical Protuberance

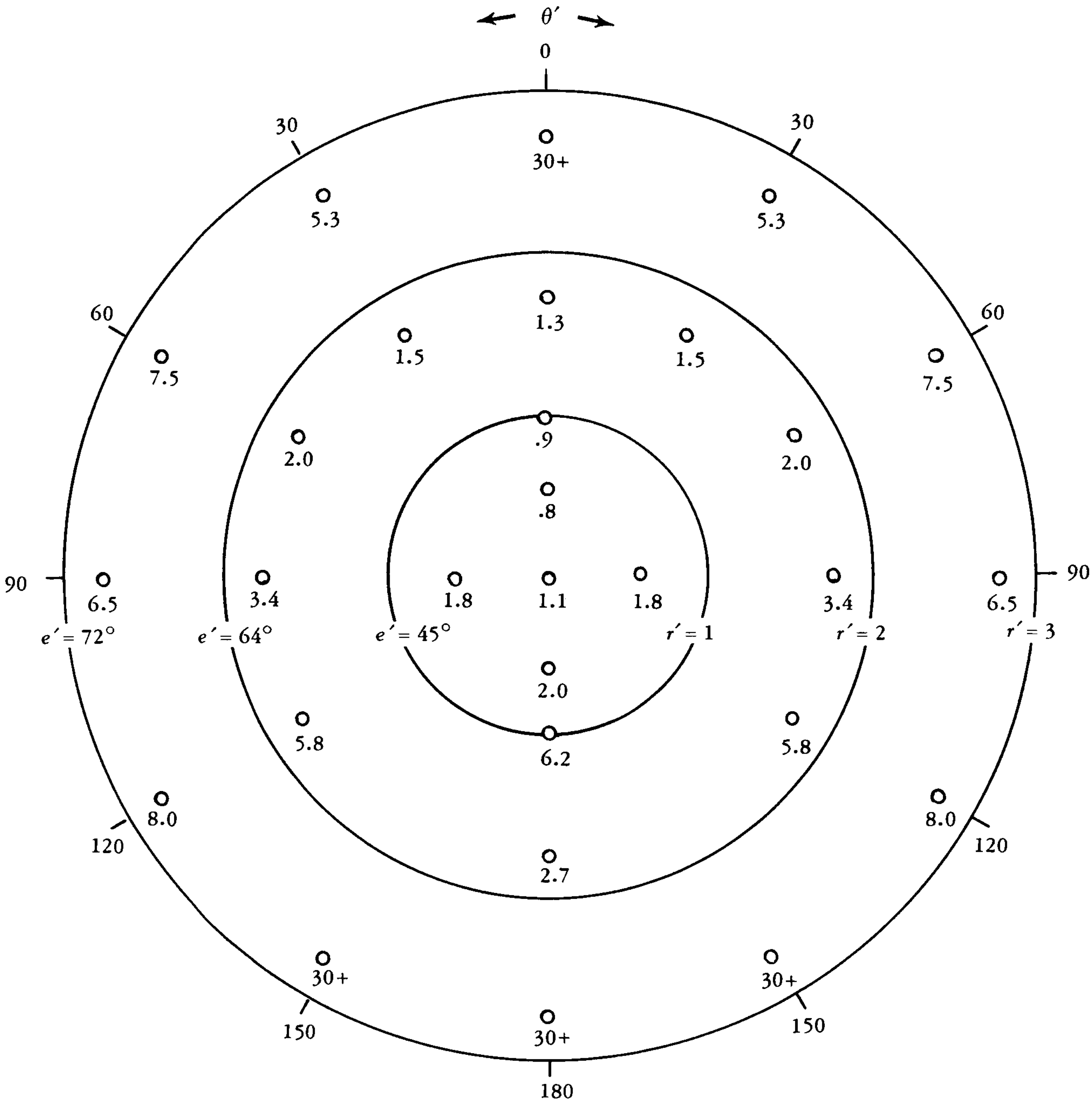

Figure 11. Threshold Concial Protuberance Height (h')

1. Observer altitude (h) = 1,000 ft.
2. Slope (β) = 15 deg.
3. Illumination (E) = 11.4 cd/m^2 (full earthshine).
4. Normal albedo ($'\rho$) = 0.065 (lunar maria area)
5. Incidence angle (i') = 70 deg (equivalent to 70 deg E or W lunar equatorial longitude).

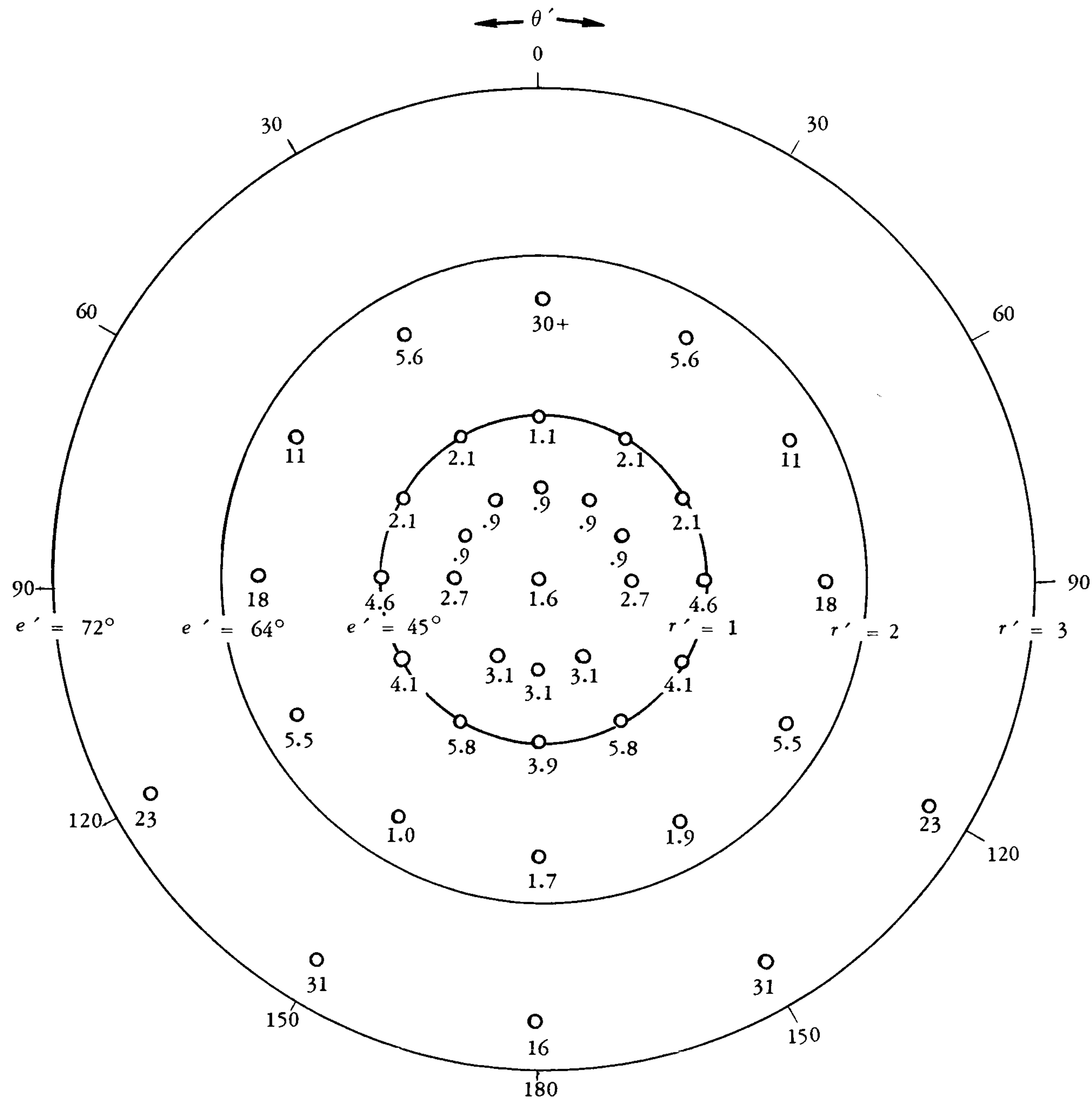

Figure 12. Threshold Concial Protuberance Height ($h.'$)

1. Observer altitude (h) = 1,000 ft.
2. Slope (β) = 15 deg.
3. Illumination (E) = 11.4 cd/m^2 (full earthshine).
4. Normal albedo (ρ) = 0.065 (lunar maria area).
5. Incidence angle (i') = 60 deg (equivalent to 60 deg E or W lunar equatorial longitude).

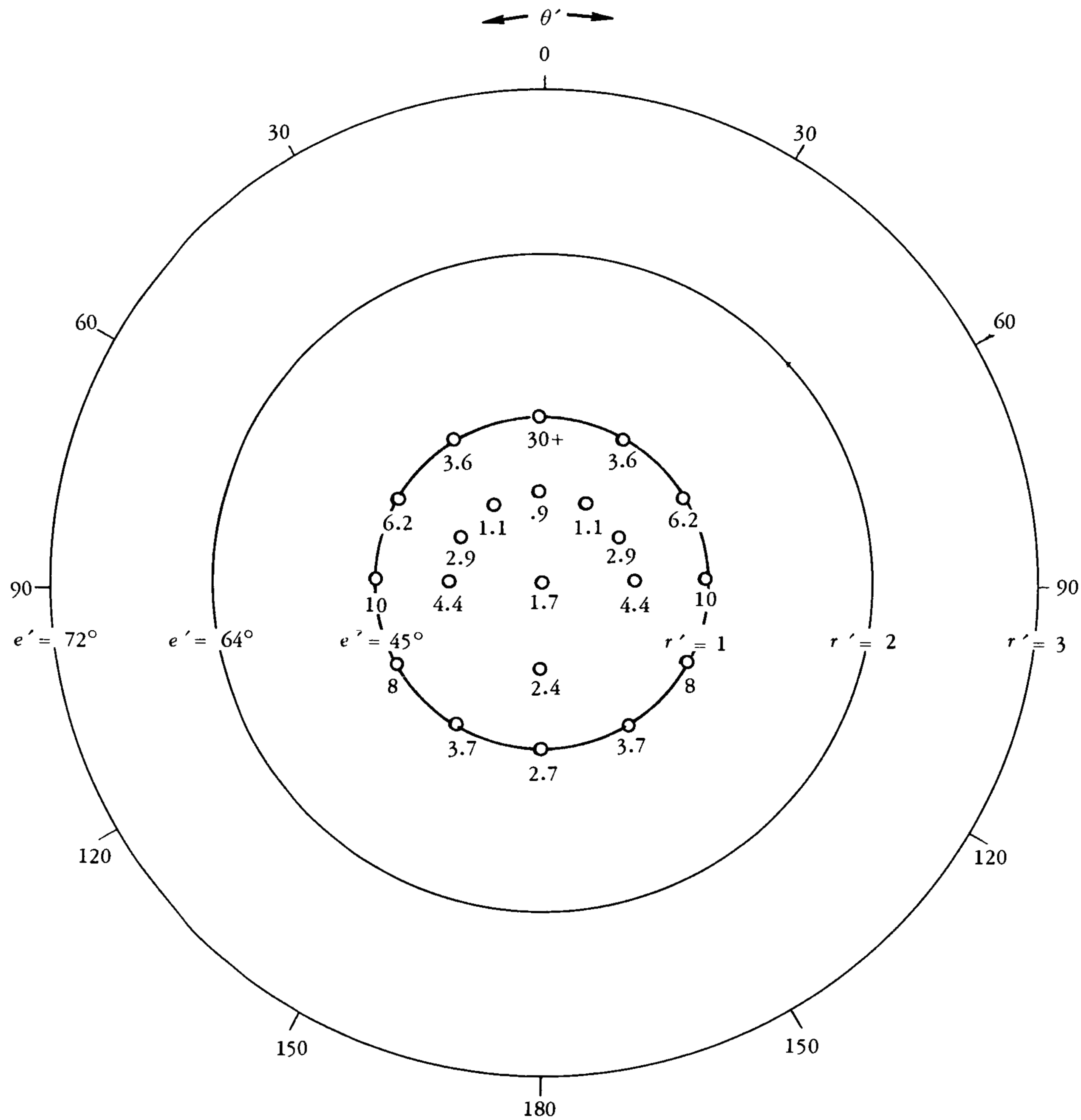

Figure 13. Threshold Conical Protuberance Height (h)

1. Observer altitude (h) = 1,000 ft.
2. Slope (β) = 15 deg.
3. Illumination (E) = 11.4 cd/m^2 (full earthshine).
4. Normal albedo (ρ) = 0.065 (lunar maria area).
5. Incidence angle (i') = 50 deg (equivalent to 50 deg E or W lunar equatorial longitude).

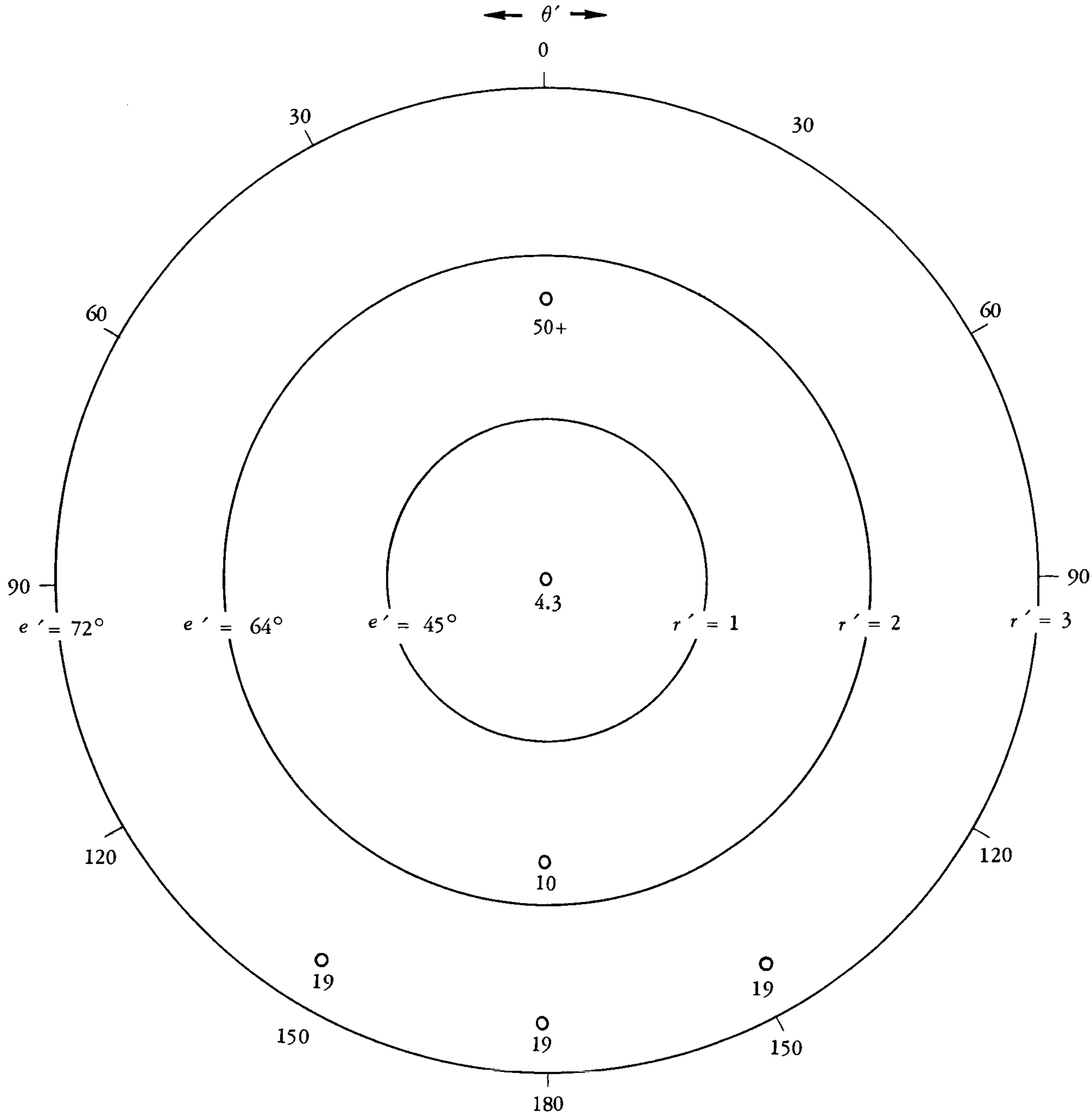

Figure 14. Threshold Conical Protuberance Height (*h*)

1. Observer altitude (*b*) = 1,000 ft.
2. Slope (β) = 15 deg.
3. Illumination (*E*) ≈ 11.4 cd/m ^{2} (full earthshine).
4. Normal albedo (β) = 0.065 (lunar maria area).
5. Incidence angle (i') = 40 deg (equivalent to 40 deg E or W lunar equatorial longitude).

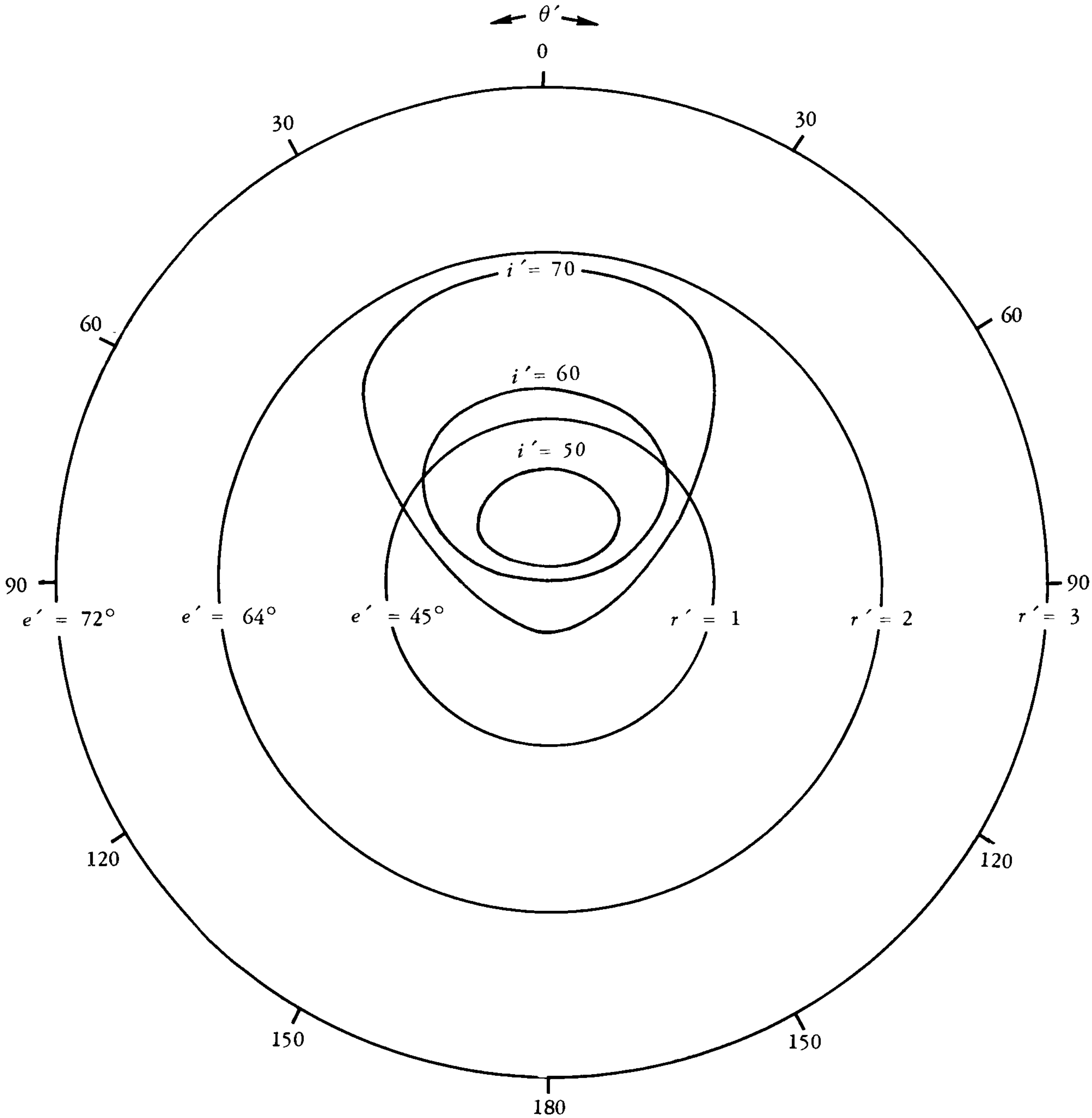

Figure 15. Contours of Constant Threshold Conical Protuberance Height (h' = 1.6 ft)

1. Observer altitude (h) = 1,000 ft.
2. Slope (β) = 15 deg.
3. Illumination (E) = 11.4 cd/m ^{2} (full earthshine).
4. Normal albedo (ρ) = 0.065 (lunar maria area).
5. Incidence angle (i') equivalent to E or W lunar equatorial longitude.

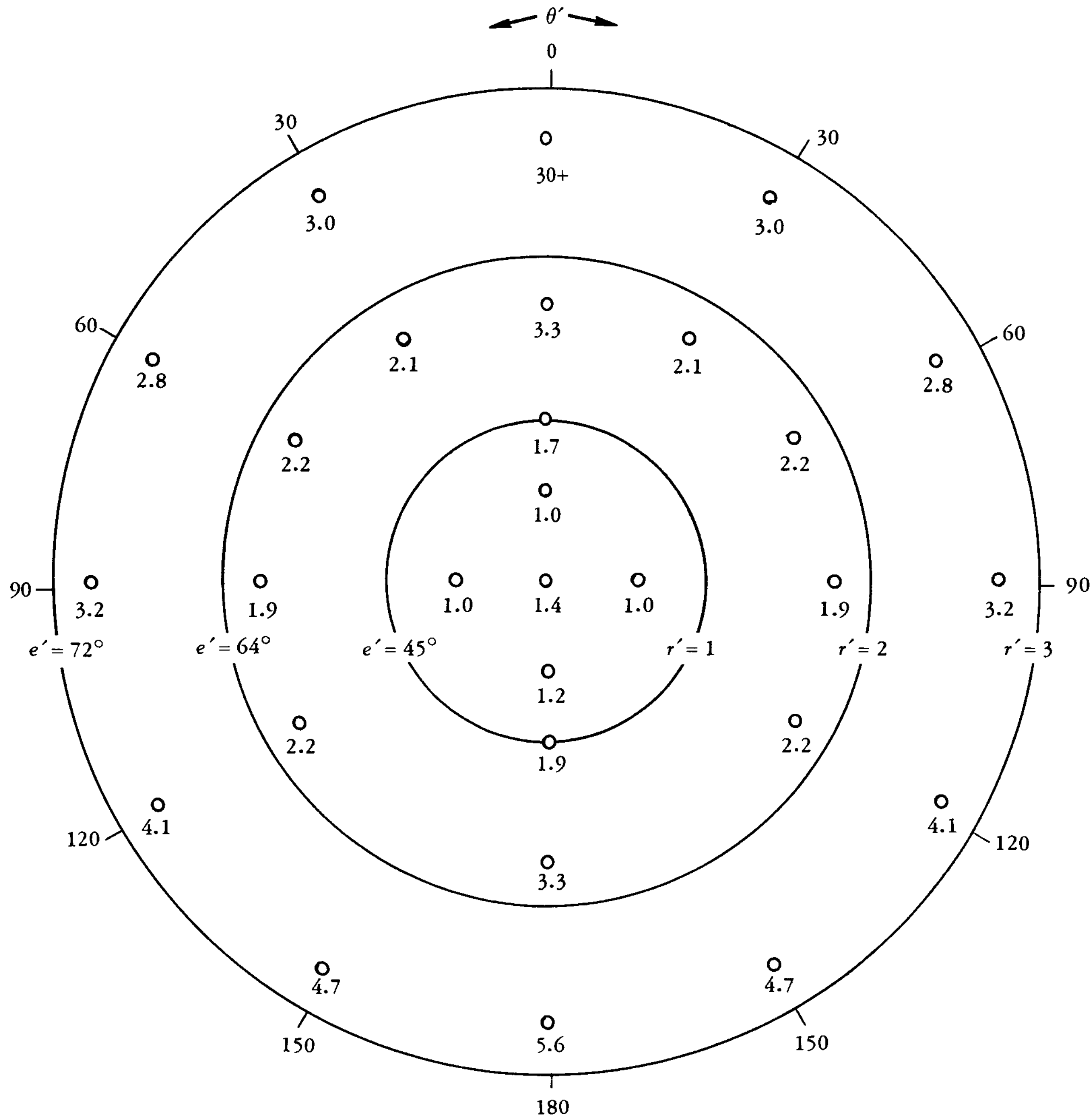

Figure 16. Threshold Spherical Protuberance Height (h')

1. Observer altitude (h) = 1,000 ft.
2. Illumination (E) = 11.4 cd/m^2 (full earthshine).
3. Normal albedo (ρ) = 0.065 (lunar maria area).
4. Incidence angle (i') = 70 deg (equivalent to 70 deg E or W lunar equatorial longitude

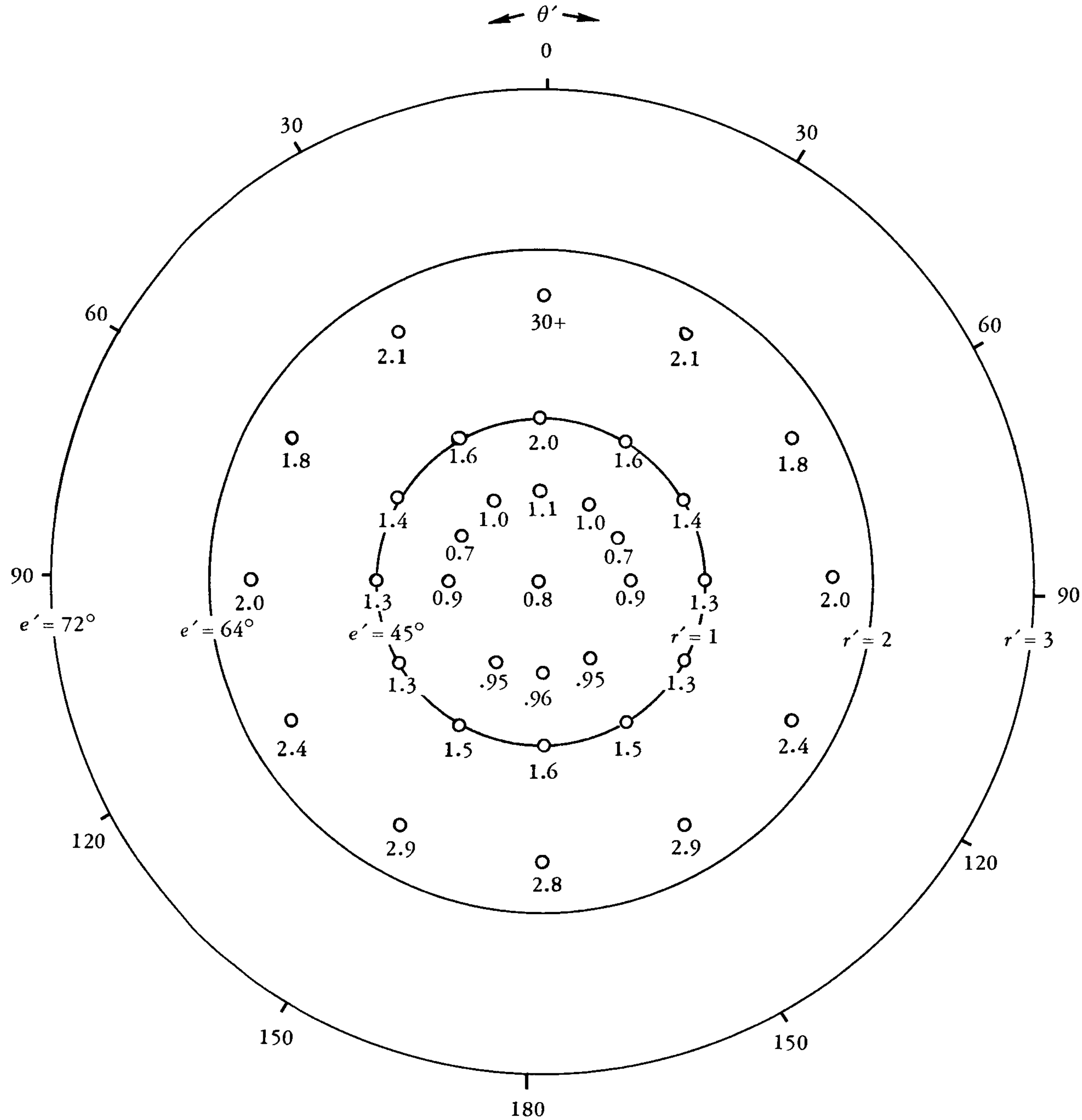

Figure 17. Threshold Spherical Protuberance Height (h')

1. Observer altitude (h) =1,000 ft.
2. Illumination (E)=11.4 cd/m ^{2}(full earthshine)
3. Normal albedo (ρ) = 0.065 (lunar maria area)
4. Incidence angle (i') = 60 deg (equivalent to 60 deg E or W lunar equatorial longitude).

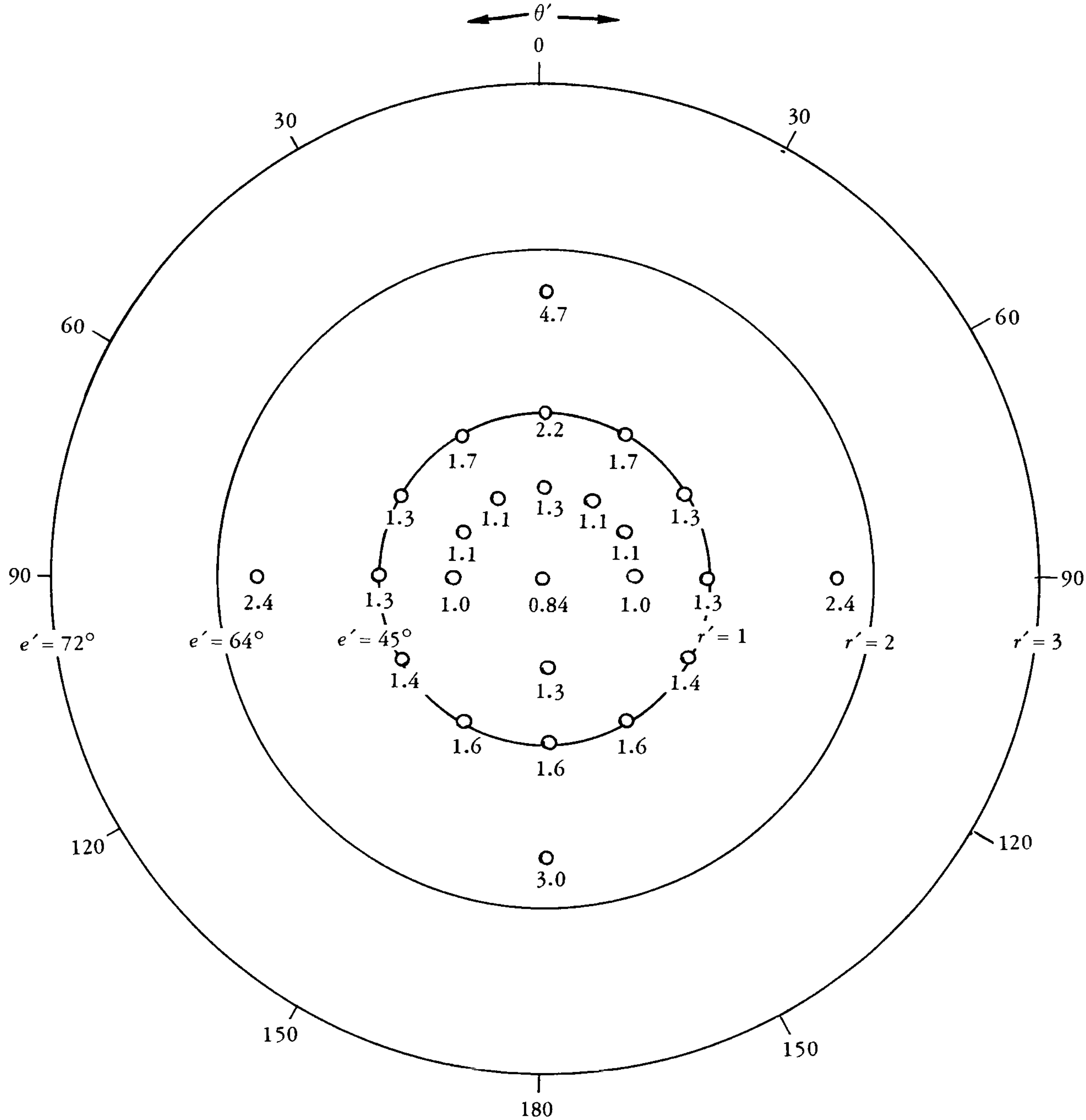

Figure 18. Threshold Spherical Protuberance Height (*h*)

1. Observer altitude (b) = 1,000 ft.
2. Illumination (b) = 11.4 cd/m^2 (full earthshine).
3. Normal albedo (ρ) = 0.065 (lunar maria area).
4. Incidence angle (i') = 50 deg (equivalent to 50 deg E or W lunar equatorial longitude).

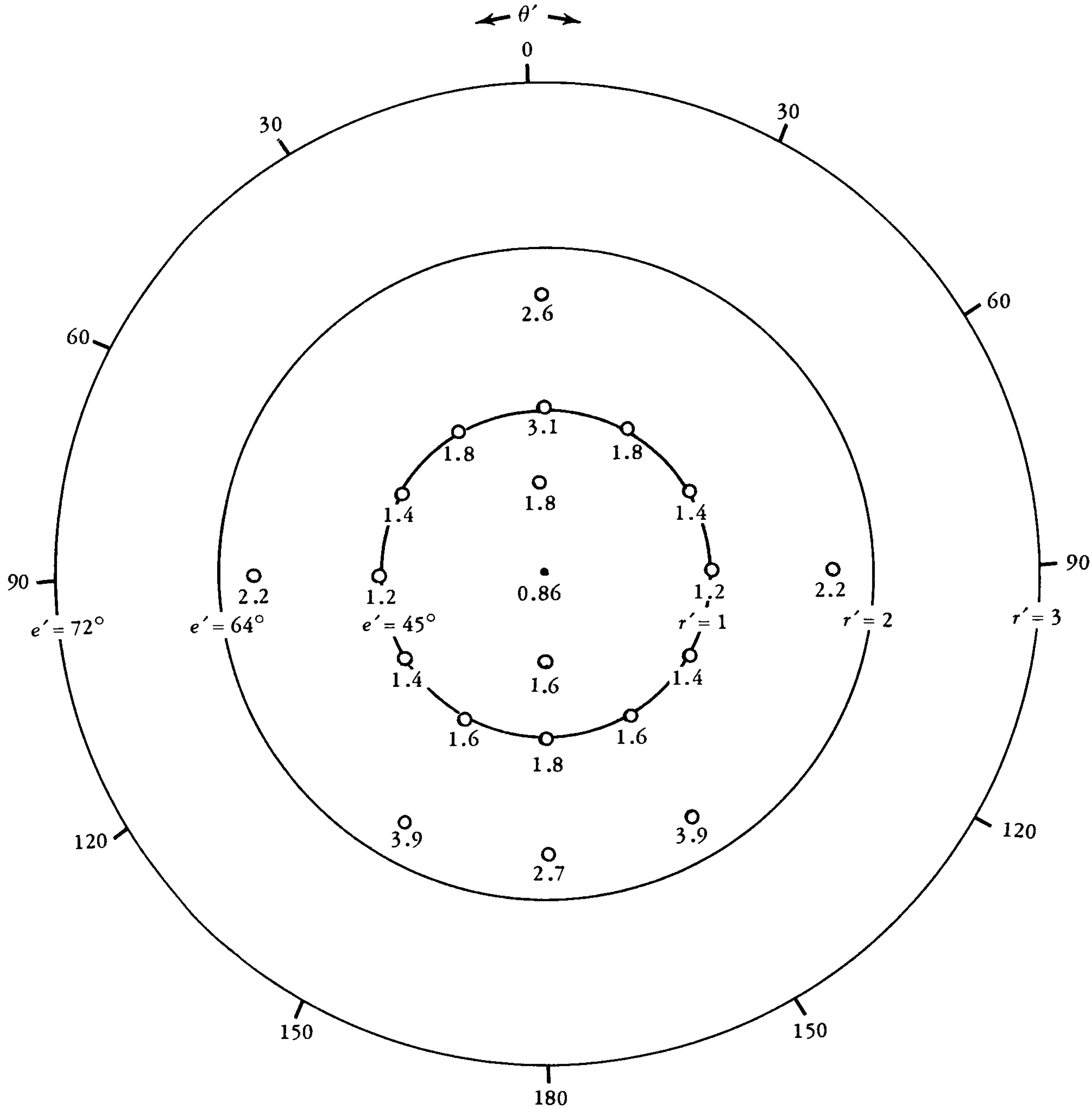

Figure 19. Threshold Spherical Protuberance Height (h')

1. Observer altitude (h) = 1,000 ft.
2. Illumination (E) = 11.4 cd/m^2 (full earthshine).
3. Normal albedo (ρ) = 0.065 (lunar maria area).
4. Incidence angle (i') = 40 deg (equivalent to 40 deg E or W lunar equatorial longitude).

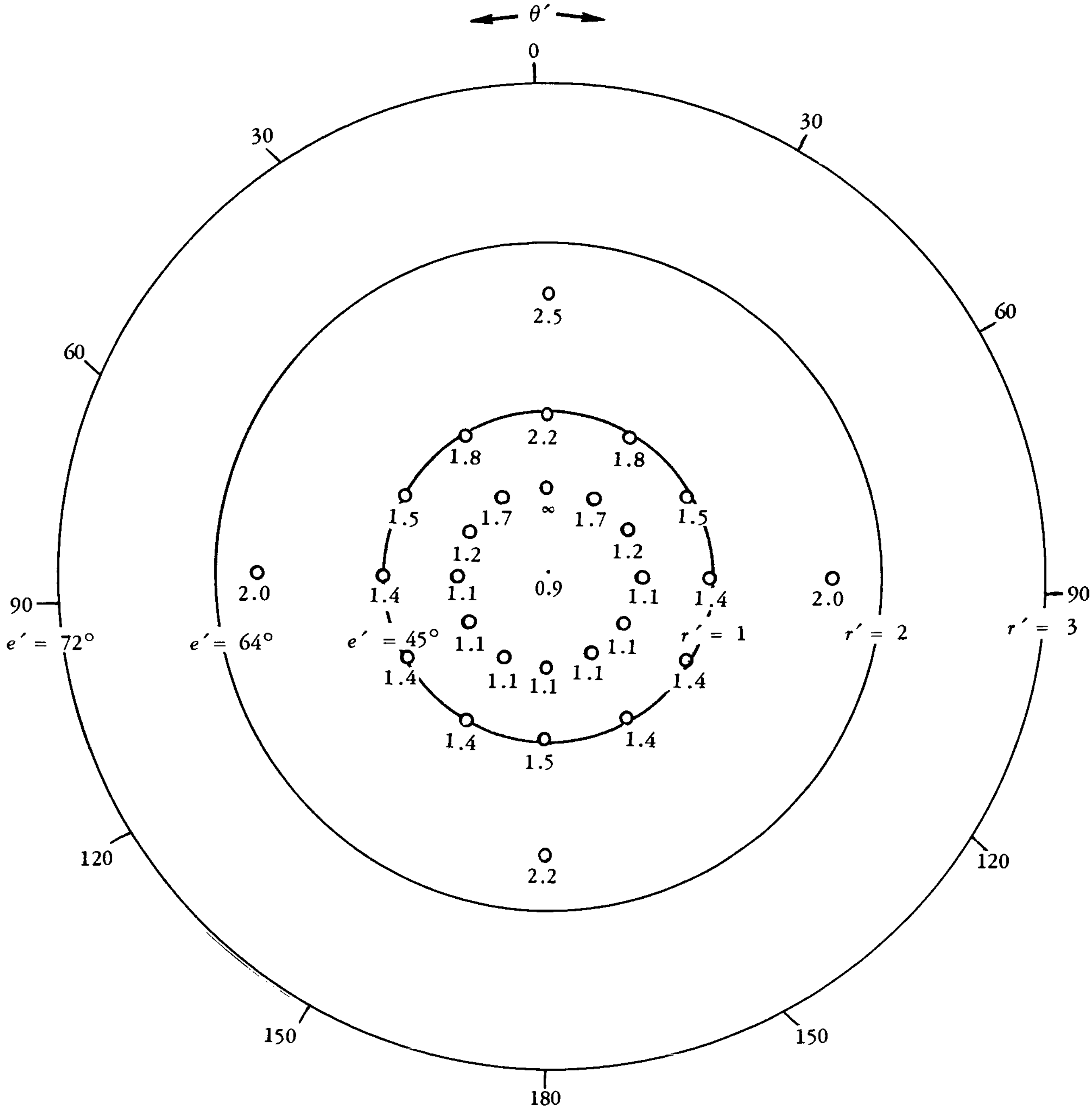

Figure 20. Threshold Sperical Protuberance Height (h')

1. Observer altitude (h) = 1,000 ft.
2. Illumination (E) = 11.4 cd/m^2 (full earthshine).
3. Normal albedo (ρ) = 0.065 (lunar maria area).
4. Incidence angle (i') = 30 deg (equivalent to 30 deg E or W lunar equatorial longitude).

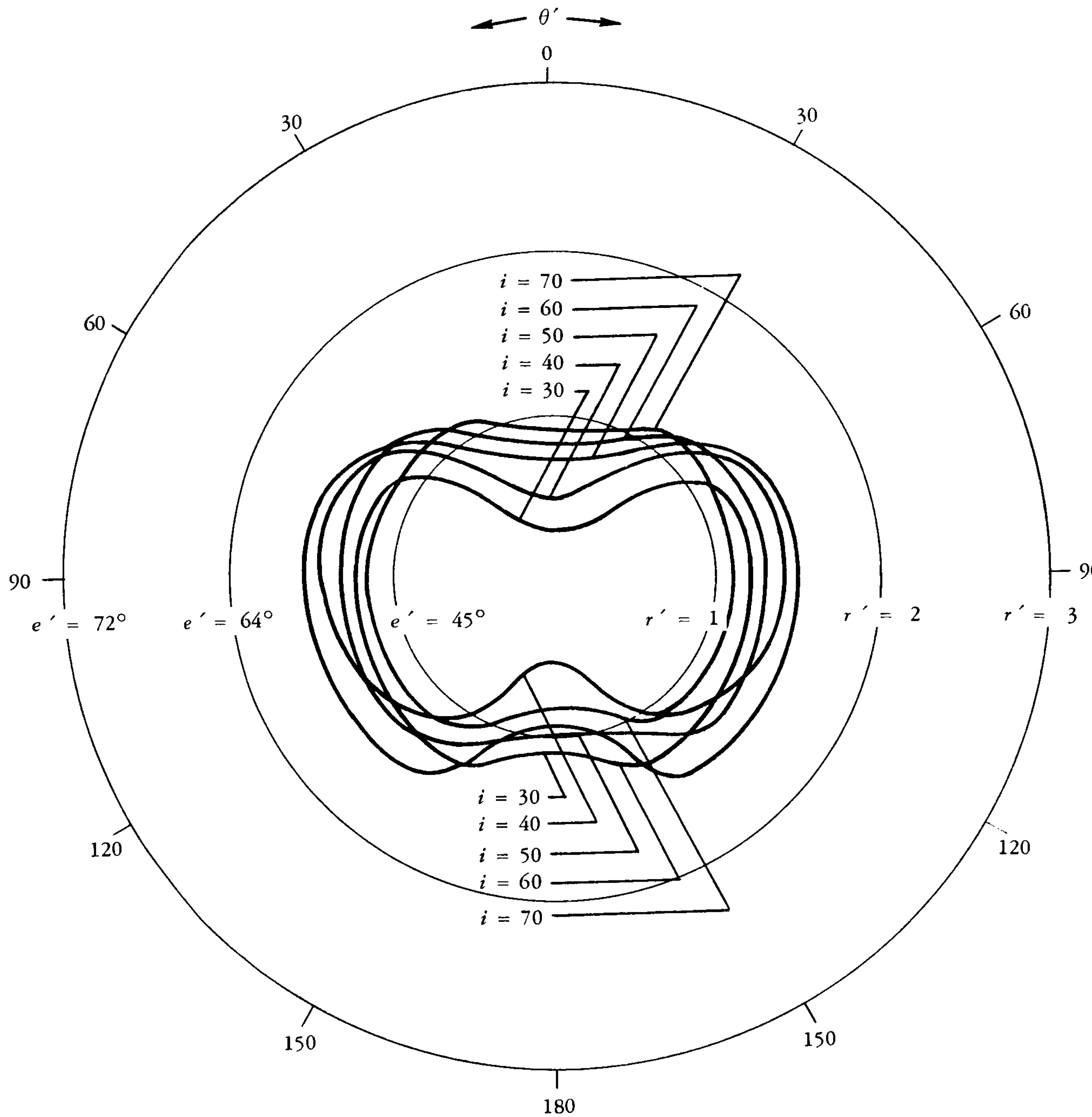

Figure 21. Contours of Constant Threshold Spherical Protuberance Height (h' = 1.6 ft)

1. Observer altitude (h) = 1,000 ft.
2. Illumination (E) = 11.4 cd/m ^{2} (full earthshine).
3. Normal albedo (ρ) = 0.065 (lunar maria area).
4. Incidence angle (i') equivalent to E or W lunar equatorial longitude.

APPENDIX A
SAMPLE CALCULATION FOR CONES

Problem: Find threshold cone height h'.

Given:

$h = 1{,}000$ ft
$i' = 50$ deg
$\theta' = 60$ deg
$e' = 45$ deg
$\beta = 15$ deg
$E = 11.4$ cd/m ^{2} (full earthshine)
$\rho = 0.065$ (lunar maria normal albedo)
$K = 13.7$ deg^2
$F = 3.44 \times 10^3$ min/rad^{-1}
$a = 0.64$

Find g:

$g = \cos^{-1}$ $(1 + \cos\theta' \tan i' \tan e')$ $\cos i' \cos e'$ (from Eq. IV–1)
$g = \cos^{-1}$ $1 + \cos\theta' (1.19)$ (0.455)
$g = 43$ deg

Find $\propto$:

$|\propto'| = |\tan^{-1} [(\cos i'/\cos e') - \cos g]/\sin g|$ (from Eq. IV–3)
$|\propto'| = |\tan^{-1} [0.909 - \cos g]/\sin g|$
$\propto' = -15$ deg

Find γ:

$\gamma = \cos^{-1} (\cos e'/\cos \propto')$ (from Eq. IV–5)
$\gamma = \cos^{-1} (0.707/\cos \propto')$
$\gamma = 43$ deg

Find $\Delta\propto$:

$\Delta\propto = \tan^{-1} (\tan \beta/\cos \gamma)$ (from Eq. IV–4)
$\Delta\propto = \pm 20$ deg

Find $\propto_H$:

$\propto_H = \propto' - \Delta\propto$ (from Eq. IV–2)
$\propto_H = -35$ deg

Find $\propto_L$:

$\propto_L = \propto' + \Delta\propto$ (from Eq. IV–2)
$\propto_L = +5$ deg

Find ϕ_H: $\phi_H = 0.41$ (from Fig. 3)

Find ϕ_L: $\phi_L = 0.31$ (from Fig. 3)

Find ϕ_o: $\phi_o = 0.37$ (from Fig. 3)

Find ϕ_o': $\phi_o' = \phi_o + K\,\pi/\rho\,(180\text{-}g)^2$ (from Eq. VI–7)

$\phi_o' = \phi_o + 660/(180\text{-}g)^2$

$\phi_o' = 0.40$

Find ϵ': $$\epsilon' = \frac{\phi_H - \phi_L}{\phi_o'}$$

$\epsilon' = 0.24$

Find ϵ''' (ϵ' corrected for diffuse boundary and 95% detection probability):

$\epsilon''' = \epsilon'(1/20)$

$\epsilon''' = 0.012$

Find B_o': $$B_o' = \frac{E\rho}{\pi}\left[\phi_o + K\,\pi/\rho\,(180\text{-}g)^2\right]$$ (from Eq. VI–8)

$B_o' = 0.09$ lu. sterad.$^{-1}$ m.$^{-2}$

Find Φ: $\Phi = 75$ min (from Fig. 6)

Find h': $$h' = \left(\frac{h\Phi}{2F}\right)\left[\frac{1}{(\cos e')^{3/2}\tan\beta}\right]\left(\frac{1}{a}\right)^{1/2}$$ (from Eq. VIII–14)

$h' = 6.2$ ft

APPENDIX B
SAMPLE CALCULATION FOR SPHERES

Problem: Find threshold cone height h'

Given:

$h = 1{,}000$ ft

$i' = 50$ deg

$\theta' = 60$ deg

$e' = 45$ deg

$E = 11.4\ cd/m^2$ (full earthshine)

$\rho = 0.065$ (lunar maria normal albedo)

$K = 13.7\ deg^2$

$F = 3.44 \times 10^3$ min/rad [1]

Find g, $\propto$, ϕ_o, ϕ_o', B_o': Use the same technique as in Appendix A.

Find ϵ':

$$\epsilon' = \frac{\phi_o}{\phi_o + K\,\pi/\rho\,(180\text{-}g)^2} \qquad \text{(from Eq. VIII–4)}$$

$$\epsilon' = \frac{\phi_o}{\phi_o'}$$

$\epsilon' = 0.92$

Find ϵ'' (ϵ' corrected for 95% detection probability):

$\epsilon'' = \epsilon'/2$

$\epsilon'' = 0.46$

Find Φ: $\Phi = 3.3$ min (from Fig. 6)

Find h'

$$h' = \frac{h\,\Phi/F}{[\sin g \cos e'/\cos i' + (1 - \cos g)/2]^{1/2} \cos e'} \qquad \text{(from Eq. VIII–14)}$$

$h' = 1.3$ ft